Development of NFIQ 2.0

Evaluation of Potential Image Features for Quality Assessment

Version 0.5

Table of Contents

List of Figures

List of Tables

1 Introduction

According to ISO /IEC 29794-1 [1], the quality score output by a biometric quality assessment algorithm should convey a predicted utility of the biometric sample, where the utility of the biometric sample reflects its impact on the recognition performance of the biometric system. This relationship between quality and system performance is depicted in Figure 1.

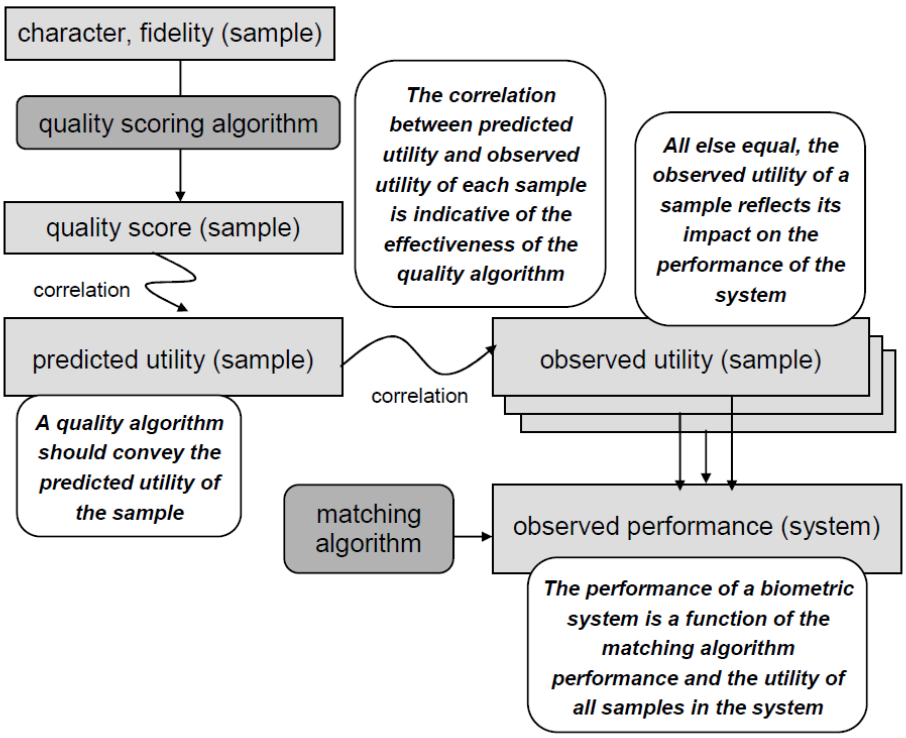

Figure 1: Relationship between quality and system performance (taken from [1])

In accordance with these requirements, the approach taken for the development of the NFIQ and the NFIQ2.0 algorithm is to train a machine learning algorithm (e.g. a neural network) to predict the utility of fingerprints from global and local structures of the fingerprint image, henceforth referred to as quality features. The potential to predict the utility heavily depends on the significance of the quality features for the image properties influencing its utility, i.e. the more indicative the quality features are for the expected biometric performance of the fingerprint, the better can an algorithm predict the utility.

Several quality features have been proposed in the literature, in particular in ISO/IEC 29794-4 [6], [12] and the NIST report on the development of the NFIQ algorithm [12], but also in other publications, e.g. [1], [2], [3], [4], [7], [10], [11] and [13].

In this document, we report on the implementation and systematic evaluation of a large number of features, including all features proposed in [6], [12] and [12], with respect to their eligibility for predicting fingerprint utility.

2 Features and Feature Extraction Methods

2.1 NFIQ1 Features

The NFIQ1 features are implemented by the NBIS package and have been used in the training of the NFIQ algorithm [12]. They are based on the minutiae output by MINDTCT and a quality map [13]. The quality map is computed on segmentation of the image into 8x8 pixel blocks. This quality map and the local image contrast are used by MINDTCT to compute a quality value for each minutia.

Feature	Description
foreground	number of blocks that are quality 1 or better
total #of minutia	number of total minutiae found in the fingerprint (using
min05	number of minutiae that have quality 0.5 or better
min06	number of minutiae that have quality 0.6 or better
min075	number of minutiae that have quality 0.75 or better
min08	number of minutiae that have quality 0.8 or better
min09	number of minutiae that have quality 0.9 or better
quality zone 1	percentage of the foreground blocks of quality map with quality =1
quality zone 2	percentage of the foreground blocks of quality map with quality =2
quality zone 3	percentage of the foreground blocks of quality map with quality =3
quality zone 4	percentage of the foreground blocks of quality map with quality =4

Table 1: Description of NFIQ1 Features.

2.2 FingerJet FX Features

2.2.1 Number of Minutiae

Origin	DigitalPersona FingerJetFX OSE
NFIQ2.0 identifier	FingerJetFX_MinutiaeCount
Also known as	MinutiaeCount

Description

This value expresses the number of minutia extracted by the open source edition of DigitalPersona's FingerJetFX algorithm.

2.2.2 Fingerprint Quality

Origin	DigitalPersona FingerJetFX OSE
NFIQ2.0 identifier	FingerJetFX_FingerprintQuality
Also known as	FingerprintQuality

Description

This value expresses the quality of the fingerprint image returned by the open source edition of DigitalPersona's FingerJetFX algorithm.

Notes

The FingerJetFX algorithm constantly returns the value 86. Hence, this feature can be considered irrelevant.

2.2.3 Average Minutiae Quality

Origin	DigitalPersona FingerJetFX OSE
NFIQ2.0 identifier	FingerJetFX_AverageMinutiaeQuality
Also known as	AverageMinutiaeQuality

Description

This value expresses the average (arithmetic mean) quality of all returned minutiae by the open source edition of DigitalPersona's FingerJetFX algorithm.

2.2.4 Minutiae Quality 0

Origin	DigitalPersona FingerJetFX OSE
NFIQ2.0 identifier	FingerJetFX_MinutiaeQuality_0
Also known as	MinutiaeQuality 0

Description

This value expresses the percentage of all detected minutiae quality values that have a value of 0 are greater than 100. (Absolute number of minutiae quality values that are 0 or >100 divided by the absolute number of detected minutiae).

2.2.5 Minutiae Quality 1

Origin	DigitalPersona FingerJetFX OSE
NFIQ2.0 identifier	FingerJetFX_MinutiaeQuality_1
Also known as	MinutiaeQuality 1

Description

This value expresses the percentage of all detected minutiae quality values that are in the range from 1 until 10 (Absolute number of minutiae quality values that are >= 1 and <= 10 divided by the absolute number of detected minutiae).

2.2.6 Minutiae Quality 2

Origin	DigitalPersona FingerJetFX OSE
NFIQ2.0 identifier	FingerJetFX_MinutiaeQuality_2
Also known as	MinutiaeQuality 2

Description

This value expresses the percentage of all detected minutiae quality values that are in the range from 11 until 20 (Absolute number of minutiae quality values that are >= 11 and <= 20 divided by the absolute number of detected minutiae).

2.2.7 Minutiae Quality 3

Origin	DigitalPersona FingerJetFX OSE
NFIQ2.0 identifier	FingerJetFX_MinutiaeQuality_3
Also known as	MinutiaeQuality 3

Description

This value expresses the percentage of all detected minutiae quality values that are in the range from 21 until 30 (Absolute number of minutiae quality values that are >= 21 and <= 30 divided by the absolute number of detected minutiae).

2.2.8 Minutiae Quality 4

Origin	DigitalPersona FingerJetFX OSE
NFIQ2.0 identifier	FingerJetFX_MinutiaeQuality_4
Also known as	MinutiaeQuality 4

Description

This value expresses the percentage of all detected minutiae quality values that are in the range from 31 until 40 (Absolute number of minutiae quality values that are >= 31 and <= 40 divided by the absolute number of detected minutiae).

2.2.9 Minutiae Quality 5

Origin	DigitalPersona FingerJetFX OSE
NFIQ2.0 identifier	FingerJetFX_MinutiaeQuality_5
Also known as	MinutiaeQuality 5

Description

This value expresses the percentage of all detected minutiae quality values that are in the range from 41 until 50 (Absolute number of minutiae quality values that are >= 41 and <= 50 divided by the absolute number of detected minutiae).

2.2.10 Minutiae Quality 6

Origin	DigitalPersona FingerJetFX OSE
NFIQ2.0 identifier	FingerJetFX_MinutiaeQuality_6
Also known as	MinutiaeQuality 6

Description

This value expresses the percentage of all detected minutiae quality values that are in the range from 51 until 60 (Absolute number of minutiae quality values that are >= 51 and <= 60 divided by the absolute number of detected minutiae).

2.2.11 Minutiae Quality 7

Origin	DigitalPersona FingerJetFX OSE
NFIQ2.0 identifier	FingerJetFX_MinutiaeQuality_7
Also known as	MinutiaeQuality 7

Description

This value expresses the percentage of all detected minutiae quality values that are in the range from 61 until 70 (Absolute number of minutiae quality values that are >= 61 and <= 70 divided by the absolute number of detected minutiae).

2.2.12 Minutiae Quality 8

Origin	DigitalPersona FingerJetFX OSE
NFIQ2.0 identifier	FingerJetFX_MinutiaeQuality_8
Also known as	MinutiaeQuality 8

Description

This value expresses the percentage of all detected minutiae quality values that are in the range from 71 until 80 (Absolute number of minutiae quality values that are >= 71 and <= 80 divided by the absolute number of detected minutiae).

2.2.13 Minutiae Quality 9

Origin	DigitalPersona FingerJetFX OSE
NFIQ2.0 identifier	FingerJetFX_MinutiaeQuality_9
Also known as	MinutiaeQuality 9

Description

This value expresses the percentage of all detected minutiae quality values that are in the range from 81 until 90 (Absolute number of minutiae quality values that are >= 81 and <= 90 divided by the absolute number of detected minutiae).

2.2.14 Minutiae Quality 10

Origin	DigitalPersona FingerJetFX OSE
NFIQ2.0 identifier	FingerJetFX_MinutiaeQuality_10
Also known as	MinutiaeQuality 10

Description

This value expresses the percentage of all detected minutiae quality values that are in the range from 91 until 100 (Absolute number of minutiae quality values that are >= 91 and <= 100 divided by the absolute number of detected minutiae).

2.3 hda Features

2.3.1 Notation

X	Image width in pixels (horizontal)
Y	Image height in pixels (vertical)
$I(x,y)$	Image location where $I(1,1)$ denotes the pixel in the upper left corner
M	Number of blocks horizontally
N	Number of blocks vertically
$V(i,j)$	Image block where $V(1,1)$ denotes the block in the upper left corner

2.3.2 Frequency Domain Analysis

Origin	ISO/IEC TR 29794-4:2010 (ISO/IEC, 2010) – Clause 6.2.2.3
NFIQ2.0 identifier	FDA_#
Short acronym	

Description

The Frequency Domain Analysis algorithm operates in a block-wise manner. A signature of the ridge-valley structure is extracted and the DFT is computed to determine the frequency of the sinusoid following the ridge-valley structure.

Extracting the ridge-valley signature

$$T(x) = \frac{1}{2r+1}\sum_{k=-r}^{r} I(x,k)$$

Computing the Frequency Domain Analysis score

$$Q_{FDA} = \frac{A(F_{max}) + 0.3(A(F_{max}-1) + A(F_{max}+1))}{\sum_{F=1}^{N/2} A(F)}$$

Algorithm

1. For each block determine the dominant ridge flow orientation
2. Rotate the block such that the dominant ridge flow is perpendicular to the x-axis
3. Crop regions of block such that no invalid regions are included in the block
4. Calculate the mean pixel intensity value $T(x)$ for the block to extract the ridge-valley structure
5. Calculate the Fourier spectrum of $T(x)$
6. Discard the DC component of $T(x)$ and determine the term F_{max} with the highest magnitude $A(F_{max})$
7. The final Frequency Domain Analysis score is the mean of scores assigned to foreground blocks.

Notes

The value of Q_{FDA} is undefined if $F_{max} = 1$ or $F_{max} = A(end)$ as $A(0)$ is not a valid index. Workaround in that case is to set $Q_{FDA} = 1$.

Processing

Input

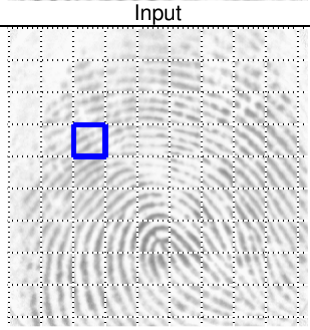

Input with block grid and current block marked in blue

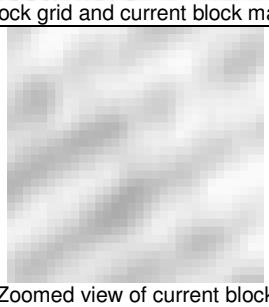

Zoomed view of current block

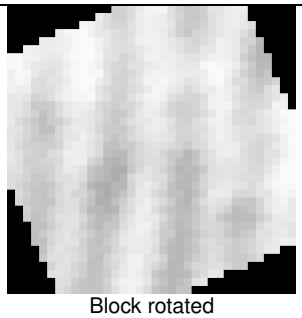

Block rotated

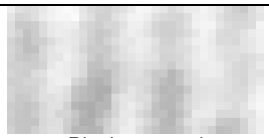

Block cropped

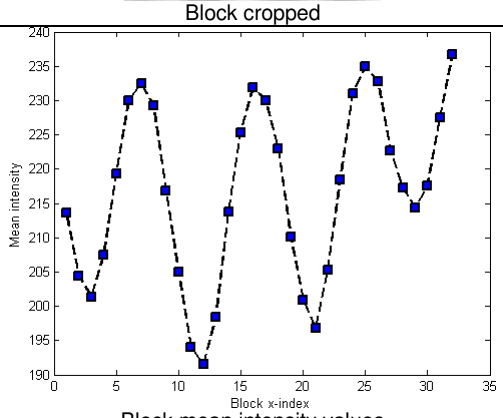

Block mean intensity values

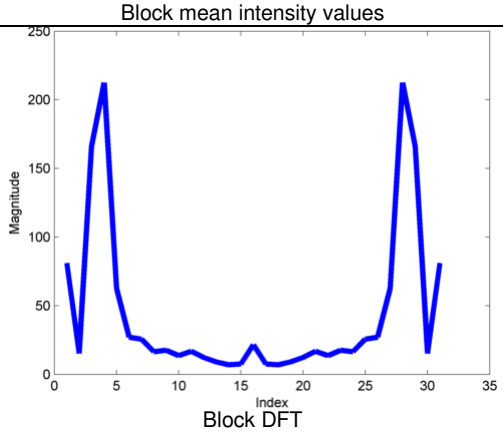

Block DFT

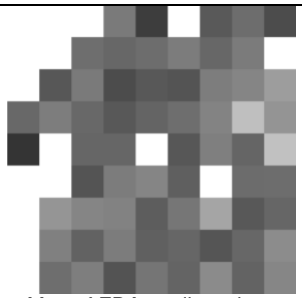

Map of FDA quality values

2.3.3 Gabor

Origin	Olsen, Xu, Busch, Gabor Filters as Candidate Quality Measure for NFIQ 2.0 in ICB 2012
NFIQ2.0 identifier	GABOR_#
Short acronym	GAB

Description

The Gabor quality metric operates on a per-pixel basis by calculating the standard deviation of the Gabor filter bank responses. The size of the filter bank is used to determine a number of filters oriented evenly across the half circle. The strength of the response at a given location corresponds agreement between filter orientation and frequency in the location neighborhood. For areas in the fingerprint image with a regular ridge-valley pattern there will be a high response from one or a few filter orientations. In areas containing background or unclear ridge-valley structure the Gabor response of all orientations will be low and constant.

Variables

σ_x	2D Gaussian standard deviation in x-direction
σ_y	2D Gaussian standard deviation in y-direction
n	Size of filter bank , orientations of the gabor wave
f	Gabor filter frequency

The Gabor filter

The general form of the complex 2D Gabor(Daugman, 1985) filter h_{cx} in the spatial domain is given by:

$$h_{Cx}(x, y; f, \theta, \sigma_x, \sigma_y) = \exp\left(-\frac{1}{2}\left(\frac{x_\theta^2}{\sigma_x^2} + \frac{y_\theta^2}{\sigma_y^2}\right)\exp(j2\pi f x_\theta)\right)$$

where

$x_\theta = x \sin\theta + y \cos\theta$

$y_\theta = x \cos\theta - y \sin\theta$

and *f* is the frequency (cycles/pixel) of the sinusoidal plane wave along the orientation θ. The size of the Gaussian smoothing window is determined by σ_x, σ_y. The filter bank size *n* is used to compute the differently oriented Gabor filters composing the filter bank. The computation of θ given *n* is as follows:

$$\theta = \frac{k-1}{n\pi}, k = 1, \dots, n$$

Algorithm

1. Convolve input image with a 2D Gaussian kernel with $\sigma = 1$ and subtract it from the input image to give $\bar{I}$
2. Compute the Gabor response of $\bar{I}$ for each orientation θ
3. Convolve the magnitude (complex modulus) of each Gabor response with a 2D Gaussian kernel with $\sigma = 4$
4. Compute the standard deviation of the Gabor magnitude response values at each location yielding a map of standard deviations.
5. Sum the map of standard deviations and normalize according to number of sample points (typically image size) to produce the final Gabor quality score.

Recommendations

For 500ppi images the following settings are reasonable:

$\sigma_x = \sigma_y = 6$

$f = 0.1$

$n = 4$

Processing

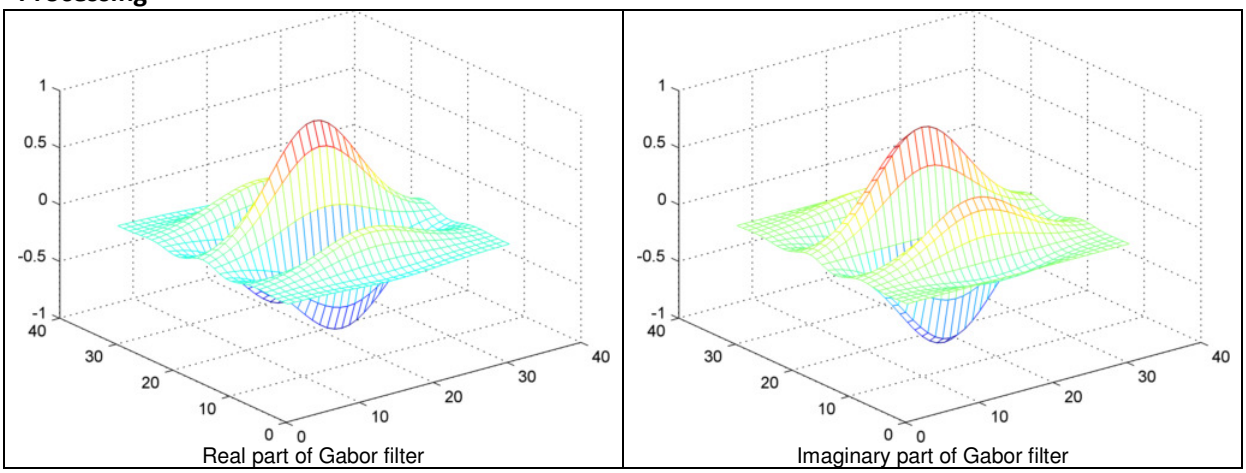

Real part of Gabor filter

Imaginary part of Gabor filter

Input (FVC2000 Db1A 1_1.bmp)

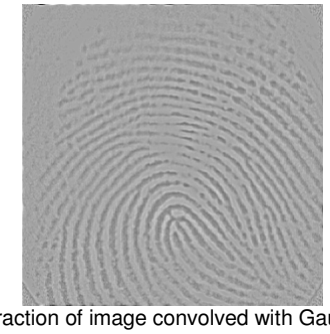

Subtraction of image convolved with Gaussian.

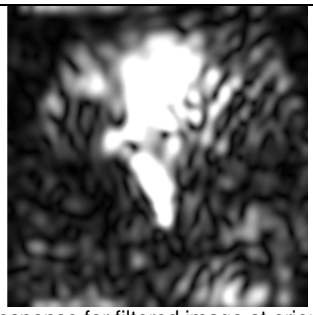

Gabor response for filtered image at orientation 0

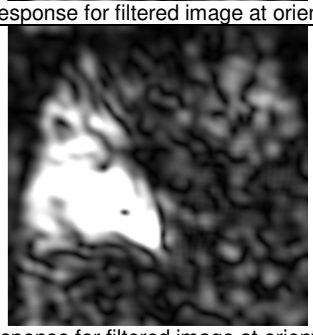

Gabor response for filtered image at orientation 1/4

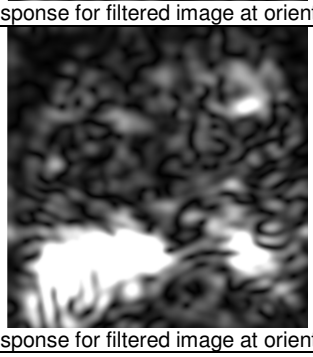

Gabor response for filtered image at orientation 2/4

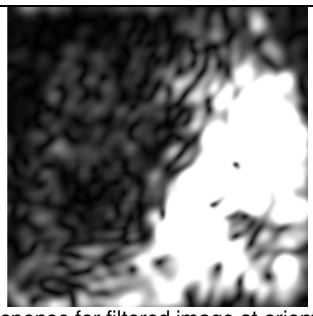

Gabor response for filtered image at orientation 3/4

Gaussian filtered Gabor response for filtered image at orientation 3/4

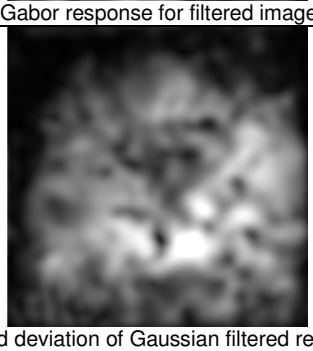

Standard deviation of Gaussian filtered responses

2.3.4 Gabor Segment

Origin	
NFIQ2.0 identifier	GS_#
Short acronym and alternate identifier	GSG, GaborSeg

Description

Same as Gabor with the exception that the image is initially convolved with a 2D Gaussian kernel with $\sigma = 8$ instead of $\sigma = 1$. Additionally a segmentation to 2 levels is applied before computing the final quality score.

Segment to two levels

Segmenting the map of standard deviations into two levels is done by first determining the cumulative distribution function for pixel intensity values. Next a threshold is determined such that the probability of a pixel belonging to background is the same as that for belonging to the foreground.

Algorithm

1. Convolve input image with a 2D Gaussian kernel with $\sigma = 8$
2. Compute the Gabor response of the image for each orientation
3. Convolve the magnitude (complex modulus) of each Gabor response with a 2D Gaussian kernel with $\sigma = 4$
4. Compute the standard deviation of the Gabor magnitude response values at each location yielding a map of standard deviations.
5. Segment the standard deviation map into two levels.

6. Sum the map standard deviations and normalize according to number of sample points (typically image size) to produce the final Gabor quality score.

2.3.5 Gabor Shen

Origin	L. Shen, A. C. Kot, and W. M. Koo. Quality measures of fingerprint images. In AVBPA, 2001
NFIQ2.0 identifier	GSh_#
Short acronym	GSH

Description

Gabor based metric separating blocks into two classes: good and bad. Quality is the ratio between foreground blocks and blocks marked as good.

Algorithm

1. Compute the Gabor response of $\bar{I}$ for each orientation θ
2. Computed the standard deviation of the Gabor magnitude response values at each location yielding a map of standard deviations.
3. Divide the map of standard deviations into blocks of size $b * b$
4. Compute the mean value of each block μ_i
5. Determine the set of blocks, B_F, belonging to the foreground as those where $\mu_i > T_b$
6. Determine the set of blocks, B_P, which are of poor quality as those where $(\mu_i > T_b) \wedge (\mu_i < T_q)$
7. The final score $Q_{GABORSHEN}$ is determined as the ratio between B_F and B_P.

Recommendations

Suggested by Shen et. al.:

$\sigma_x = \sigma_y = 4$

$f = 0.12$

$n = 8$

$b = 30$

T_b and T_q are manually determined according to dataset.

Processing

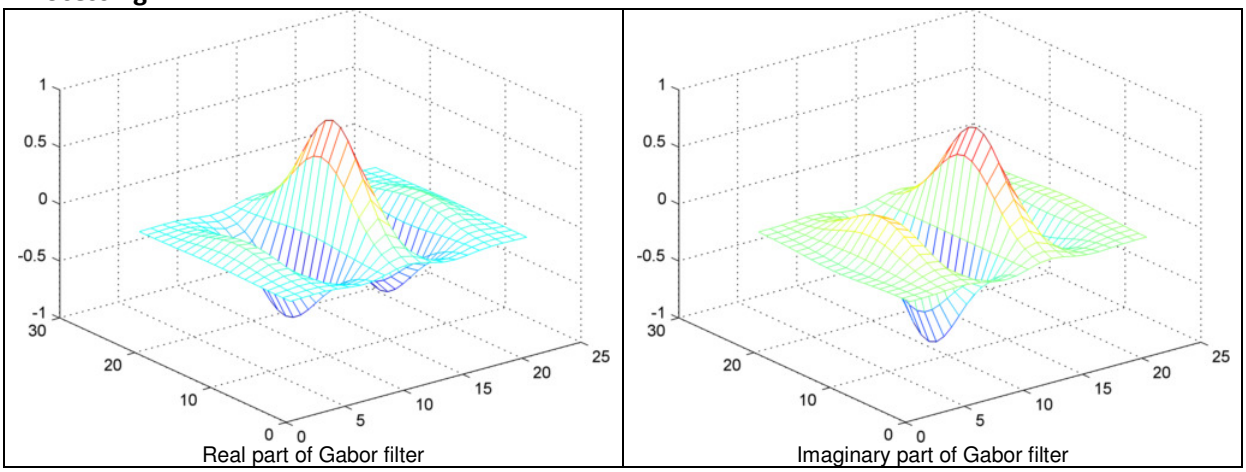

Real part of Gabor filter

Imaginary part of Gabor filter

Input

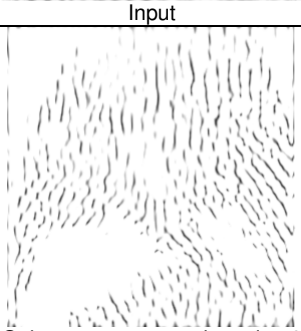

Gabor response at orientation 0

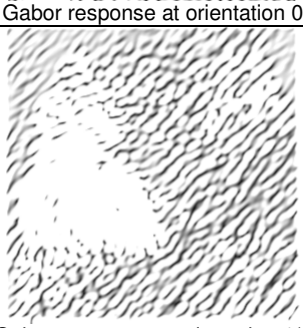

Gabor response at orientation 1/4

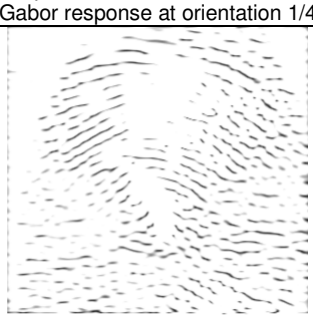

Gabor response at orientation 2/4

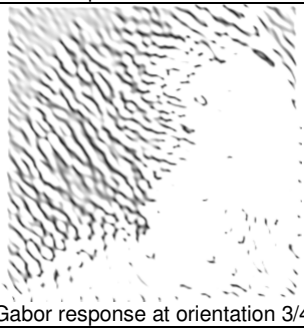

Gabor response at orientation 3/4

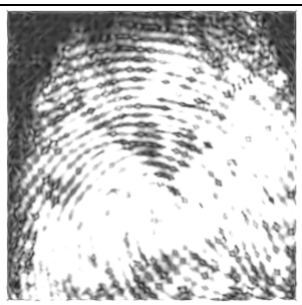

Standard deviation of filter responses

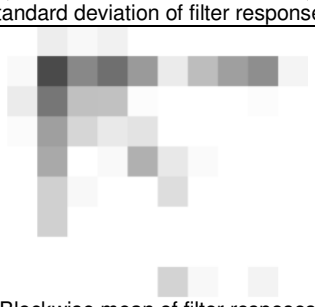

Blockwise mean of filter resposes

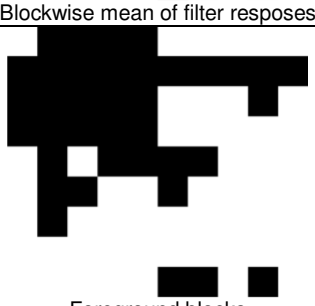

Foreground blocks

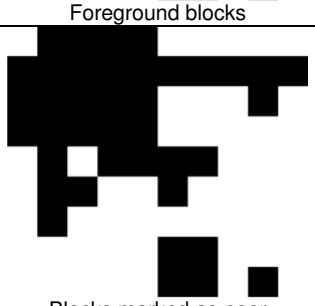

Blocks marked as poor

2.3.6 Local Clarity Score

Origin	ISO/IEC TR 29794-4:2010 (ISO/IEC, 2010) – Clause 6.2.2.2
NFIQ2.0 identifier	LCS_#
Short acronym and alternate identifier	LCS, Ridge-valley Structure

Description

Local Clarity Score (LCS) computes the block wise clarity of ridge and valleys by applying linear regression to determine a gray-level threshold, classifying pixels as ridge or valley. A ratio of misclassified pixels is determined by comparing with the normalized ridge and valley width of that block.

Computing the average profile of a block

Given the block V_2 the average profile is obtained by

$$V_3(x) = \frac{\sum_{y=1}^{M} V_2(x,y)}{M}$$

where M is the height of the block.

Determining the proportion of misclassified pixels

For a block V_2 there are v_T pixels in the valley region and v_B pixels in the valley region with intensity lower than a threshold DT. Similarly there are r_T pixels in the ridge region and r_B pixels in the ridge region with intensity lower than a threshold DT. α and β are expressions of these ratios.

$$\alpha = \frac{v_B}{v_T}$$

$$\beta = \frac{r_B}{r_T}$$

Determining the normalized ridge and valley width

The normalized valley width $\overline{W_v}$ and the normalized ridge width $\overline{W_r}$ are determined

$$\overline{W_v} = \frac{W_v}{\left(\frac{S}{125}\right)W^{max}}$$

$$\overline{W_r} = \frac{W_r}{\left(\frac{S}{125}\right)W^{max}}$$

where S is the scanner resolution in dpi, W^{max} is the estimated ridge or valley width for an image with 125 dpi resolution, and W_v and W_r are the observed valley and ridge widths. According to [] $W^{max} = 5$ is reasonable for 125 dpi resolution.

Computing the Local Clarity Score

The final quality score is computed using the average value of α and β in valid ridge and valley regions:

$$Q_{LCS} = \begin{cases} \left(1 - \left(\frac{\alpha+\beta}{2}\right)\right) * 100, & \left(W_v^{nmin} < \overline{W_v} < W_v^{nmax}\right) \wedge \left(W_r^{nmin} < \overline{W_r} < W_r^{nmax}\right) \\ 0, & otherwise \end{cases}$$

where W_r^{nmin} and W_v^{nmin} are the minimum values for the normalized ridge and valley width, and W_v^{nmax} and W_v^{nmax} are the maximum values for the normalized ridge and valley width.

Algorithm

1. For each block V_0 in the image determine the dominant ridge flow orientation to create an orientation line which is perpendicular to the ridge flow
2. Align V_0 such that the orientation line is horizontal to create V_1
3. From V_1 extract a block V_2 which is centered around the orientation line
4. Compute the average profile V_3 of V_2
5. Determine a threshold DT by applying linear regression on V_3
6. Determine the proportion of misclassified pixels β and α in the ridge and valley regions
7. Determine the normalized ridge width and valley width W_r and W_v.
8. Compute the final quality score Q_{LCS}.

Further Comments

Particular regions inherent in a fingerprint will negatively affect Q_{LCS}. For example, ridge endings and bifurcations or areas with high curvature such as those commonly found in core and delta points.

Processing

Input

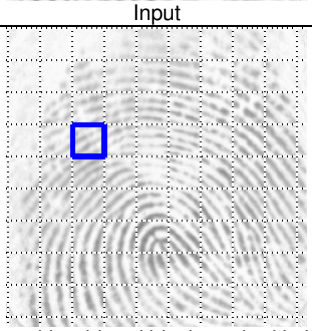

Input with grid and block marked in blue

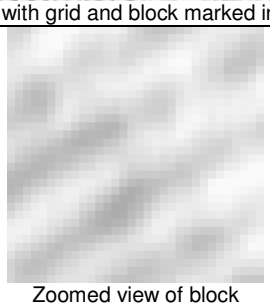

Zoomed view of block

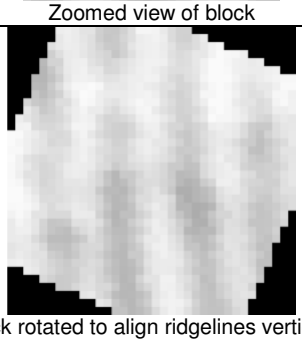

Block rotated to align ridgelines vertically

Extracted section of the block

Projected mean gray intensity values

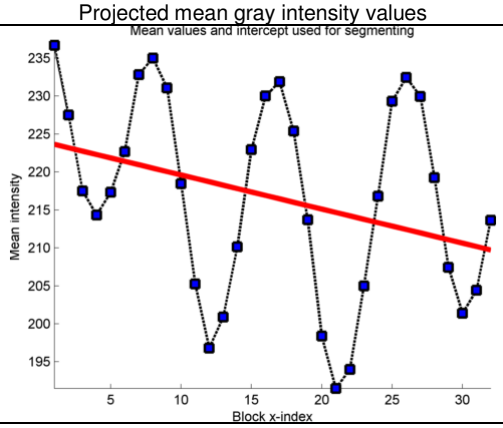

Ridge-valley profile as found by mean values. Red line indicates the threshold for ridge-valley separation.

Ridge-valley segmentation. Ridges shown in black, valleys in white. The mean intensity values are shown above for comparison.

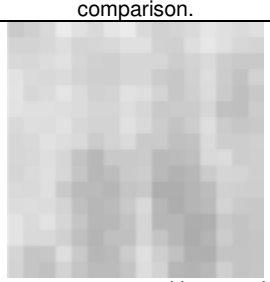

Ridge areas composed into one block.

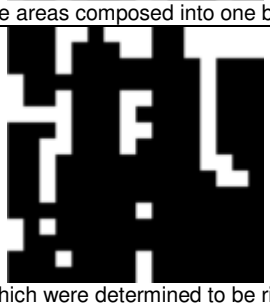

Shown in white are the parts of the fingerprint which were determined to be ridge but do not belong to ridge as defined by the threshold.

Valley areas composed into one block.

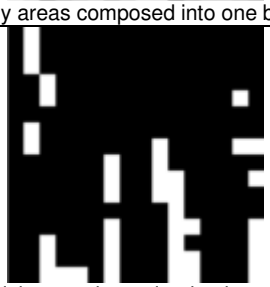

Shown in white are the parts of the fingerprint which were determined to be valley but do not belong to valley as defined by the threshold.

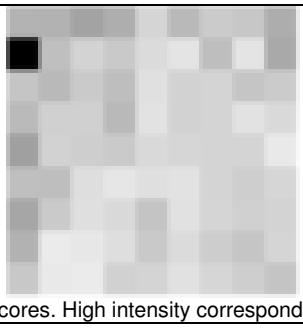

Map of local clarity scores. High intensity corresponds to high local clarity.

2.3.7 Mu

Origin	
NFIQ2.0 identifier	Mu_#
Short acronym	MUQ

Description

Mu is the mean pixel intensity value in the input image.

Algorithm

$$Q_{MU} = \frac{1}{X * Y} \sum_{y=1}^{Y} \sum_{x=1}^{X} I(x,y)$$

2.3.8 Mu Mu Block

Origin	
NFIQ2.0 identifier	MMB_#
Short acronym	MMB

Description

Mu Mu Block is the mean of the block wise mean pixel intensity value in the input image.

2.3.9 Mu Mu Sigma Block

Origin	
NFIQ2.0 identifier	MMSB_#
Short acronym	MMSB

Description

Mu Mu Sigma Block is the mean of the block wise standard deviation pixel intensity value in the input image subtracted the block wise standard deviation.

2.3.10 Mu Sigma Block

Origin	
NFIQ2.0 identifier	MSB_#
Short acronym	MSB

Description

Mu Sigma Block is the mean of the block wise standard deviation pixel intensity value in the input image.

2.3.11 Orientation Certainty Level

Origin	ISO/IEC TR 29794-4:2010 (ISO/IEC, 2010) - Clause 6.2.2.1
NFIQ2.0 identifier	OCL_#
Short acronym	OCL

Description

Orientation Certainty Level is a measure of the strength of the energy concentration along the dominant ridge flow orientation. The metric operates in a block-wise manner.

Computing the covariance matrix

The covariance matrix C is computed as:

$$C = \frac{1}{N} \sum_{N} \left\{ \begin{bmatrix} dx \\ dy \end{bmatrix} [dx \quad dy] \right\} = \begin{bmatrix} a & c \\ c & d \end{bmatrix}$$

where dx and dy represent the intensity gradient at that pixel.

Computing the eigenvalues and the final quality score

From the covariance matrix C the eigenvalues λ_{min} and λ_{max} are computed as:

$$\lambda_{min} = \frac{a + b - \sqrt{(a-b)^2 + 4c^2}}{2}$$

$$\lambda_{max} = \frac{a + b + \sqrt{(a-b)^2 + 4c^2}}{2}$$

this yields an orientation certainty level OCL:

$$OCL = 1 - \frac{\lambda_{min}}{\lambda_{max}}$$

which is a ratio in the interval $[0,1]$ where 1 is highest certainty level and 0 is lowest.

Algorithm

For each block b_i

1. Compute the intensity gradient by applying the 3x3 Sobel operators
2. Compute the covariance matrix
3. Compute the eigenvalues to obtain OCL

Finally compute the quality measure Q_{OCL} as:

$$Q_{OCL} = \frac{1}{B}\sum_{i=1}^{B} b_i$$

Processing

Input

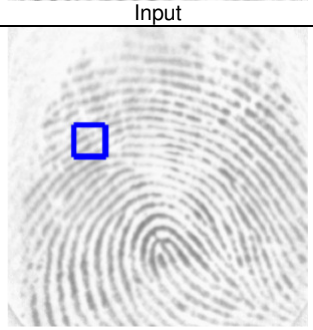

Input with current block marked

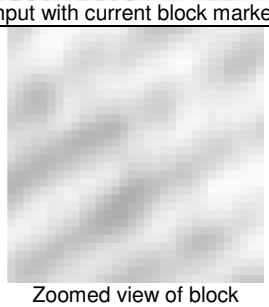

Zoomed view of block

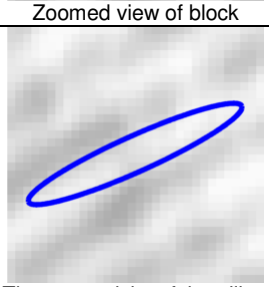

Ridge orientation indicated as an ellipse. The eccentricity of the ellipse corresponds to the orientation certainty.

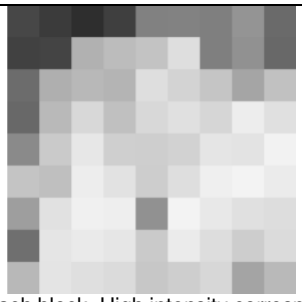

Orientation certainty level in each block. High intensity corresponds to high level of certainty.

2.3.12 Orientation Flow

Origin	ISO/IEC TR 29794-4:2010 (ISO/IEC, 2010) - Clause 6.3.2.1
NFIQ2.0 identifier	OF_#
Short acronym	OF

Description

Orientation Flow is a measure of ridge flow continuity which is based on the absolute orientation difference between a block and its neighboring blocks.

Block-wise absolute orientation difference

The ridge flow is determined as a measure of the absolute difference between a block and its neighboring blocks. The absolute difference for block $V(i,j)$ is:

$$D(i,j) = \frac{\sum_{m=-1}^{1}\sum_{n=-1}^{1}|V(i,j) - V(i-m,j-n)|}{8}$$

Local orientation quality score

The local orientation quality score $Q_{loc}(i,j)$ for the block orientation difference $D(i,j)$ is determined as:

$$Q_{loc}(i,j) = \begin{cases} 100 & , \quad D(i,j) < \theta_{min} \\ \left(1 - \frac{D(i,j) - 8}{90 - 8}\right) * 100, & D(i,j) \geq \theta_{min} \end{cases}$$

where θ_{min} is a threshold for minimum angle difference to consider.

Global orientation quality score

With $N * M$ local orientation quality score blocks the global orientation quality score is computed as:

$$Q_{OF} = \frac{1}{N * M}\sum_{i=1}^{N}\sum_{j=1}^{M} Q_{loc}(i,j)$$

Algorithm

1. Compute the absolute orientation difference $D(i,j)$ for each block $V(i,j)$
2. Compute the local orientation quality score $Q_{loc}(i,j)$ for $D(i,j)$
3. Compute the global orientation flow quality score Q_{OF}

Processing

input

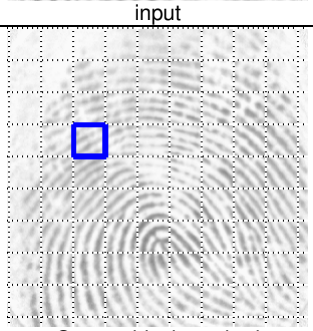

Current block marked

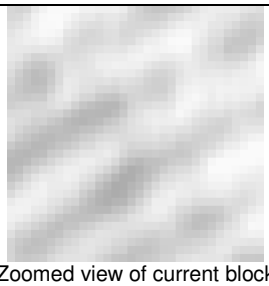

Zoomed view of current block

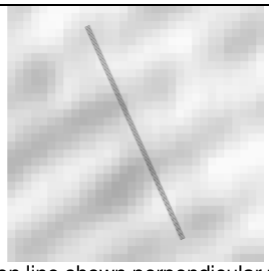

Orientation line shown perpendicular to ridges.

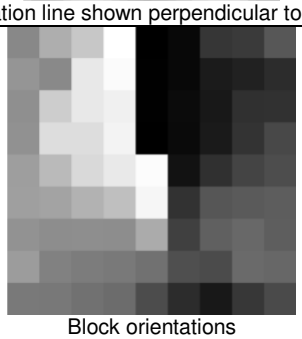

Block orientations

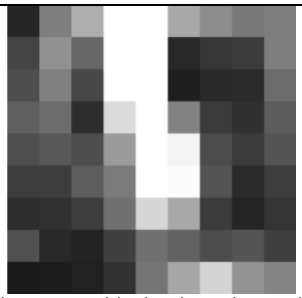

Map of differences between a block orientation and its 8-neighborhood

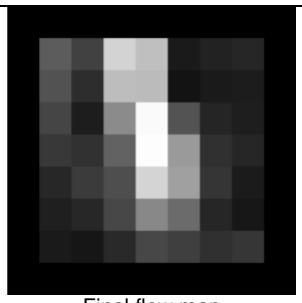

Final flow map

2.3.13 Radial Power Spectrum

Origin	ISO/IEC TR 29794-4:2010 (ISO/IEC, 2010) - Clause 6.3.2.3
NFIQ2.0 identifier	PS_#
Short acronym and alternate identifier	RPS, POW, Radial Power Spectrum

Description

The Radial Power Spectrum is a measure of maximal signal power in a defined frequency band of the global radial Fourier spectrum. Ridges can be locally approximated by means of a single sine wave, hence high energy concentration a narrow frequency band corresponds to consistent ridge structures.

Variables

r_{min}	Lower bound of frequency band
r_{max}	Upper bound of frequency band
Δ_r	Frequency bin width

The 2D Discrete Fourier Transform

The 2D discrete Fourier transform $f(x,y)$ of $I(x,y)$ is:

$$f(x,y) = \frac{1}{M*N}\sum_{m=0}^{M-1}\sum_{n=0}^{N-1} I(x,y)\exp\left(-j2\pi\left(\frac{m*x}{M}+\frac{n*y}{N}\right)\right)$$

and the magnitude of $f(x,y)$ is:

$$F(x,y) = |f(x,y)|^2$$

Magnitude of frequency bands polar coordinates

The magnitude of the annular band between r and Δ_r in the polar Fourier spectrum $F(\alpha,r)$ is computed as:

$$I(r) = \frac{\sum_{\alpha=0}^{\pi}\sum_{r}^{r+\Delta_r} F(\alpha,r)}{\sum_{\alpha=0}^{\pi}\sum_{r_{min}}^{r_{max}} F(\alpha,r)}$$

where α is the angle and r is the radius.

Determine quality score from energy distribution

The quality metric Q_{POW} is found as:

$$Q_{POW} = \max_{r\in[r_{min},r_{max}]} I(r)$$

Algorithm

1. Compute the magnitude of the 2D-DFT $F(x,y)$
2. Transform $F(x,y)$ into polar coordinates and normalize to the range of $[0,1]$
3. Determine the maximum energy to compute Q_{POW}

Process

Input

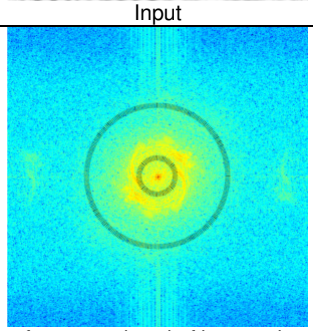

Spectrum with the frequency band of interest located between the

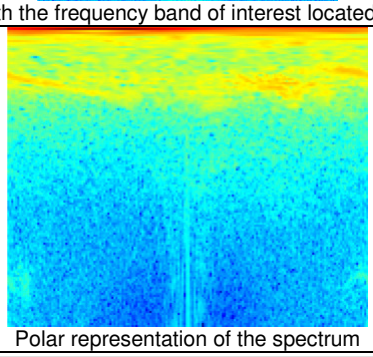

Polar representation of the spectrum

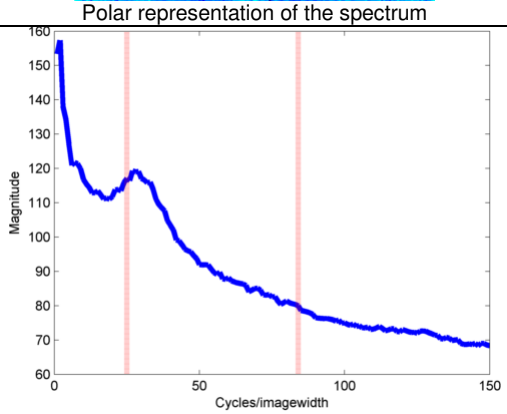

Spectrum with marked frequency of interest

2.3.14 Ridge Valley Uniformity

Origin	ISO/IEC TR 29794-4:2010 (ISO/IEC, 2010) - Clause 6.2.2.4
NFIQ2.0 identifier	RVU_#
Short acronym	RVU

Description

Ridge Valley Uniformity is a measure of the consistency of the ridge and valley widths.

Algorithm

1. For each block V_0 in the image determine the dominant ridge flow orientation to create an orientation line which is perpendicular to the ridge flow
2. Align V_0 such that the orientation line is horizontal to create V_1

3. From V_1 extract a block V_2 which is centered around the orientation line
4. Compute the average profile V_3 of V_2 to produce a vector
5. Determine a threshold DT by applying linear regression on V_3
6. Segment V_3 into two levels based on the threshold DT
7. Determine the indexes in V_3 where a change from background to foreground or foreground to background occurs. If no changes are found then return an empty ratio for that block.
8. Remove the first and last parts of V_3 to remove incomplete ridge/valleys occurring at the border of the original block. Likewise remove the corresponding changes from the change index vector.
9. If there are no changes after step 8, return an empty ratio for that block
10. Calculate the ratios between the width of ridges and valleys for the block.
11. Obtain the final quality score as the standard deviation of all ratios.

Process

Input

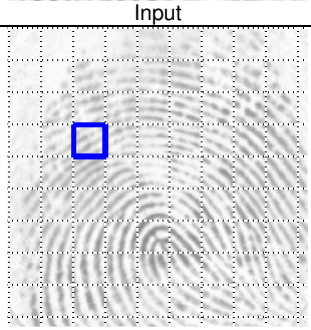

Input with block grid and current block marked

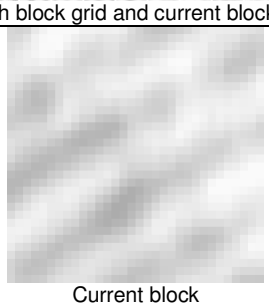

Current block

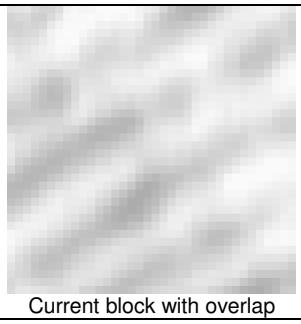

Current block with overlap

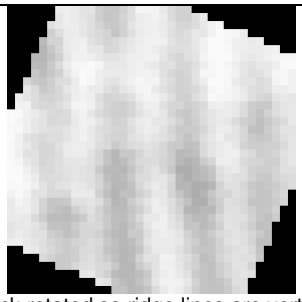

Block rotated so ridge lines are vertical

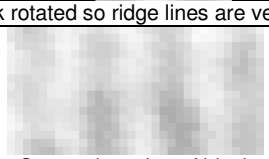

Cropped section of block

Projection of mean intensity

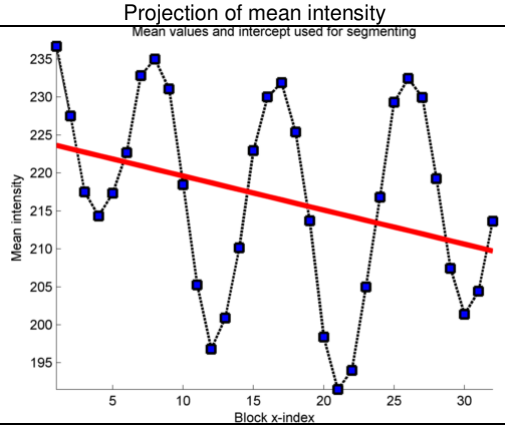

Segmentation according to thresholding. Ridges marked in black, valleys in white

Location of ridge-valley edges marked with white

Cleaned ridge-valley segmentation contains only complete ridges and valleys.

2.3.15 Sigma

Origin	
NFIQ2.0 identifier	Sigma_#
Short acronym	SIG

Description

Sigma is the standard deviation of pixel intensity values in the input image.

Algorithm

$$Q_{SIGMA} = \left(\frac{1}{X * Y - 1} \sum_{y=1}^{Y} \sum_{x=1}^{X} (I(x,y) - \bar{I})^2 \right)^{\frac{1}{2}}$$

where $\bar{I}$ is the mean pixel intensity of I.

2.3.16 Sigma Mu Block

Origin	
NFIQ2.0 identifier	SMB_#
Short acronym	SMB

Description

Sigma Mu Block is the standard deviation of the block wise mean pixel intensity value in the input image.

3 Evaluation Approach

3.1 Methodology

The following methods were used to evaluate the features:

- Determination of spearman correlation among the features and with a utility measure determined from a large number of biometric comparisons.
- Visual inspection of scatter plots.
- Computation of ROC curves resulting from a biometric application simulation, where the feature values are used to select the best fingerprint during enrolment. Details are described in Section 3.1.1.
- Computation of ERC showing the dependence of the FNMR from filtering the genuine scores by the feature values of both reference and probe images (see Section 3.1.3).

3.1.1 Spearman Correlation and Scatter Plots

We compute the spearman correlation, i.e. rank correlation, of the feature values with both the utility values and with values of other features. The utility values are computed according to ISO/IEC 29794-1 for providers 28, 63 and 83, and are used as “ground truth” metric for quality, i.e. the correlation coefficients of the feature values with utility are supposed to indicate their dependency on quality and vice-versa. The correlation coefficients with other feature’s values indicate the potential redundancy among the different features.

For the ease of reading, the correlation matrices are colored according to the absolute value of the correlation coefficient (darker color for higher absolute values) and the coefficients are shown multiplied by 100 and rounded.

In addition to correlation, scatter plots are computed with both the utility values and with values of other features. The scatter plots allow detection of more comlex dependencies than the (one dimensional) correlation.

3.1.2 Evaluation by ROC Curves

In order to evaluate how indicative a feature is for biometric performance, we simulate a biometric application using the feature values as quality assessment

criteria. In particular, we perform the following steps on a large database of fingerprints with several impressions per finger:

1. For each fingerprint, we compute a large number of genuine and impostor comparison scores.
2. For each finger, we select the impression having the highest feature value as reference fingerprint.
3. For the selected reference fingerprints, average error rates are computed from their similarity scores. In particular, from the comparison scores of the selected fingerprints accumulated genuine and impostor score distributions are computed and ROC curves are determined. The smaller the error rates are, the more eligible the utility function is to perform quality assurance with the deployed filter method and threshold. The probe fingerprints are not filtered by the feature values.
4. Steps 2 and 3 are repeated but this time, in step 2, the impression having the lowest feature value is chosen as reference image.
5. The better of the two resulting ROC curves, i.e. the ROC curve with lowest error rates is chosen as a measure for the feature.

These steps simulate an evaluation of biometric performance of a biometric system which deploys the utility function for quality assessment during enrolment.

The ROC curves were computed from the comparison scores of several providers.

For comparison, ROC curves were also computed for the case where always the first of the three impressions (with respect to their acquisition numbers) is chosen as reference fingerprint. Since the acquisition number is assumed to be unrelated to image quality, this selection criterion simulates a scenario where no quality filtering is applied at all.

3.1.3 ERC Evaluation

An error reject curve (ERC) shows the dependence of the FNMR at a fixed comparison score threshold on the extent of filtering the genuine scores by feature value of both reference and probe image. First, a comparison score threshold t is selected which results in a fixed FNMR (e.g. 10%), e.g. for which a fraction of FNMR genuine scores are equal or larger than t. Then for each feature threshold $0 \leq q \leq 1$,

all genuine scores are neglected for which the feature value of the reference image or the feature value of the probe image is below the threshold q. For the remaining genuine scores, the fraction of genuine scores equal or larger than t is determined, e.g. the FNMR resulting from filtering a q fraction of the genuine scores.

The resulting ERC can vary for different FNMR. Thus, we compute ERC for FNMR of 3% and FNMTR of 10%.

3.2 Data basis

For our experiments we use the FingerQS database of BSI, which contains 9 impressions (taken with 3 sensors) of 8784 fingers from 1098 individuals (all fingers except little fingers). In order to amplify differences between tested utility functions in the resulting error rates, we split each user-ID into 3 pseudo-IDs and assign for each finger code 3 fingerprints of this user-ID (taken by the same sensor) to each pseudo-ID. Thus, we treat the impressions of each finger as impressions of 3 different fingers. By this re-labeling, the number of user-IDs is increased by a factor of three and, at the same time, the number of fingerprints per finger is reduced by a factor of three; the reduction of impressions per finger increases the impact of variations in the utility function to the selection of the best fingerprint per finger.

The utility values are computed for three different providers (SDKs), having identifiers 28, 63 and 83. For each fingerprint and each provider, 8 genuine scores and, on average, 57.5 impostor scores are used to compute the utility values. ROC curves are also computed for all three providers. In contrast, we restrict our evaluation with ERC computed from the comparison scores of one provider (28).

3.3 Limitations

Both the correlation coefficients and the ROC curves measure to what extend the utility increases or decreases with feature values. Any non-monotonic dependency of feature values from utility is not captured. However, such monotonic dependency can be visible in the ERC and in the scatter plots.

Furthermore, since in the ROC curve method the filtering of fingerprints is performed per finger but not between impressions of different fingers, only intra-finger dependencies of feature values from utility are measured. Therefore, only influences of the quality aspect “fidelity” as defined in ISO/IEC 29794-1 [6], [12], i.e. the quality of the image with respect to the original characteristic, on the feature are captured,

and the impact of the quality aspect “character”, i.e. the eligibility of the character for biometric applications, can not be determined from the ROC curves.

4 Evaluation Results

4.1 Evaluation of the NFIQ1-Features

4.1.1.1 Correlation and Scatter Plots

The spearman correlation coefficients of the 11 NFIQ1 features are given in the following table.

	foreground	NoMinutiae	min05	min06	min075	min08	min09	QualZone1	QualZone2	QualZone3	QualZone4	util28	util63	util83
foreground	100	46	47	47	42	34	26	-19	-43	-4	25	16	2	9
NoMinutiae	46	100	49	49	50	46	35	20	18	24	-24	-7	-7	-6
min05	47	49	100	99	93	76	54	-46	-47	-47	58	33	21	26
min06	47	49	99	100	95	79	56	-45	-47	-48	58	33	21	26
min075	42	50	93	95	100	90	69	-36	-42	-45	52	31	21	26
min08	34	46	76	79	90	100	87	-25	-32	-37	41	28	19	24
min09	26	35	54	56	69	87	100	-20	-20	-31	31	23	16	20
QualZone1	-19	20	-46	-45	-36	-25	-20	100	52	66	-85	-34	-22	-27
QualZone2	-43	18	-47	-47	-42	-32	-20	52	100	39	-75	-31	-18	-25
QualZone3	-4	24	-47	-48	-45	-37	-31	66	39	100	-86	-40	-27	-31
QualZone4	25	-24	58	58	52	41	31	-85	-75	-86	100	44	29	35
util28	16	-7	33	33	31	28	23	-34	-31	-40	44	100	80	83
util63	2	-7	21	21	21	19	16	-22	-18	-27	29	80	100	82
util83	9	-6	26	26	26	24	20	-27	-25	-31	35	83	82	100

Table 2: Spearman correlation coefficients for NFIQ1 features

The highest correlation with utility are observed for (in that order)

1. Quality Zone 4,
2. Quality Zone 3,
3. Quality Zone 1,

4. min05 and min06,
5. min075.

Scatter plots of the features with provider 63 utility according to ISO 28784-1 [5] and density plots of the empirical feature distributions are shown in Appendix A.1.

4.1.1.2 ROC curve evaluation

The following table shows for each NFIQ1 feature, which selection criterion, i.e. choosing the impression with highest feature value or selecting the one with lowest feature value, results in better a ROC curve.

Feature	Abbr.	Criterion
foreground	FG	lowest
total # of minutiae	NoMin	lowest
min05	Min05	highest
min06	Min06	highest
min075	Min075	highest
min08	Min08	highest
min09	Min09	lowest
quality zone 1	QZ1	lowest
quality zone 2	QZ2	lowest
quality zone 3	QZ3	lowest
quality zone 4	QZ4	highest

Table 3: Optimal selection criteria for ROC curves

For these criteria, the ROC curves are shown in Figure 2, Figure 3 and Figure 4

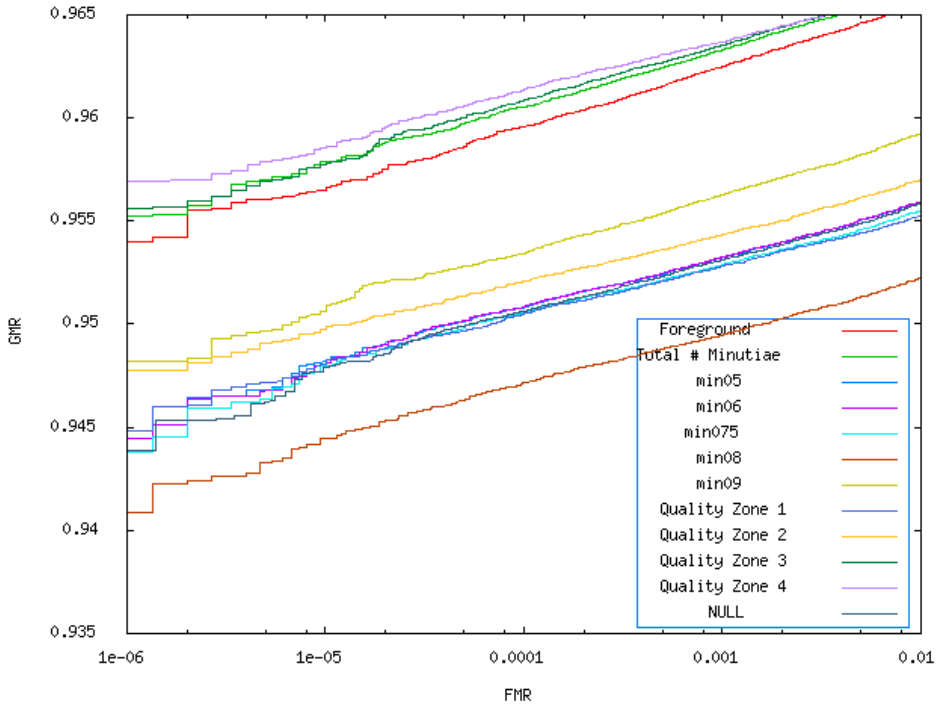

Figure 2: ROC curves of NFIQ1 features for provider 28

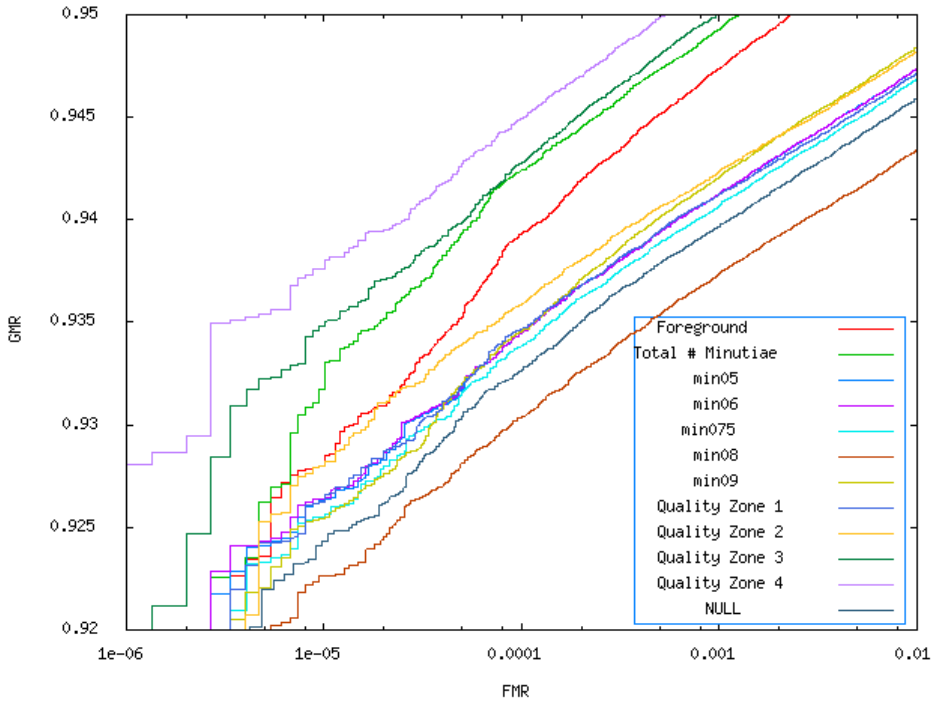

Figure 3: ROC curves of NFIQ1 features for provider 63

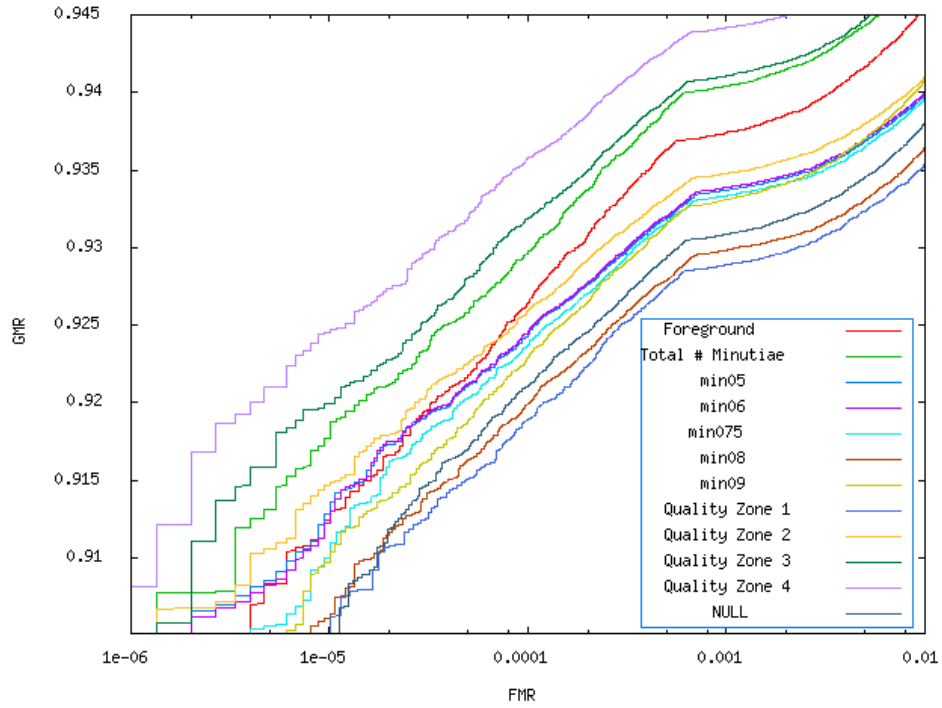

Figure 4: ROC curves of NFIQ1 features for provider 83

The following observations were made:

- Consistently, quality zone 4 performed best, followed by quality zone 3, total # of minutiae and foreground.
- Although feature min08 is positively correlated with utility, the ROC curves for both selection criteria were worse than that of a random selection (NULL feature). This finding indicates, that good quality fingerprint neither have particularly high nor particularly low feature values.
- For provider 83, feature quality zone 1 also performed worse than no quality filtering, but still choosing the impression with lowest value gave better results than selecting the one with the highest value.

Scatter plots of the features with provider 63 utility according to ISO 28784-1 [5] and density plots of the empirical feature distributions are shown in Appendix A.1.

4.1.1.3 ERC Evaluation

For the NFIQ1 features the following ERC curves were obtained. The dotted diagonal line from (0.1, 0) to (0, 0.1) for 10% FNMR and from (0.03,0) to (0.03,0) for 3% FNMR shows the ideal (and hypothetical) ERC in case of a perfect quality filtering, where scores are rejected according to their quality, starting with the lowest quality value.

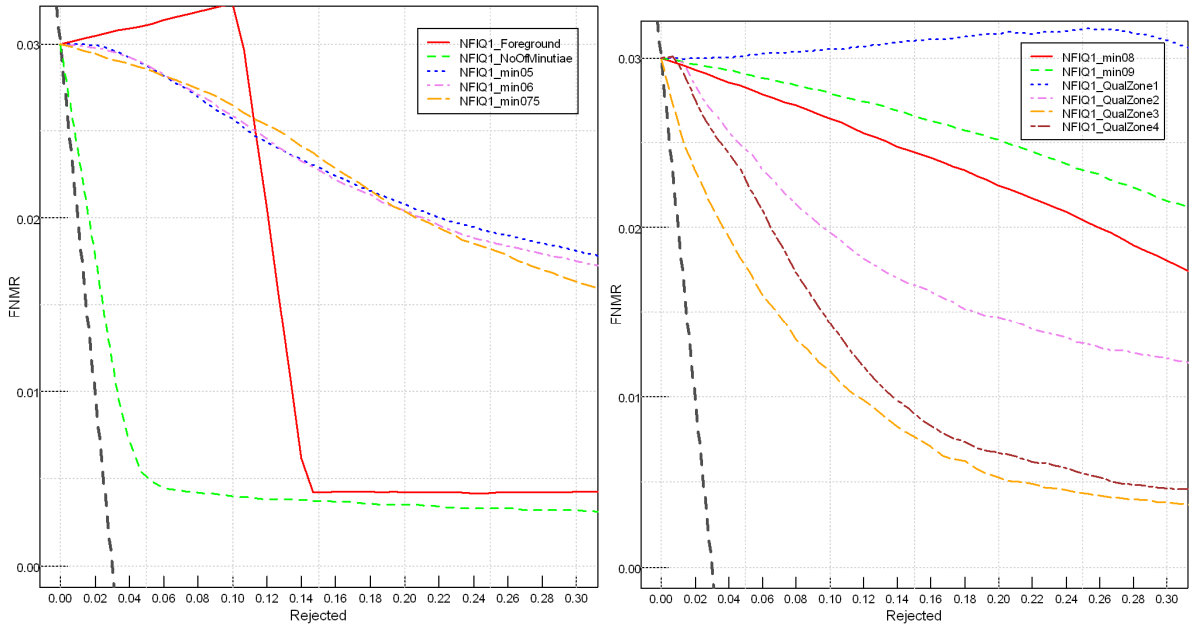

Figure 5: ERC of NFIQ 1 features at 3% FNMR for provider 28

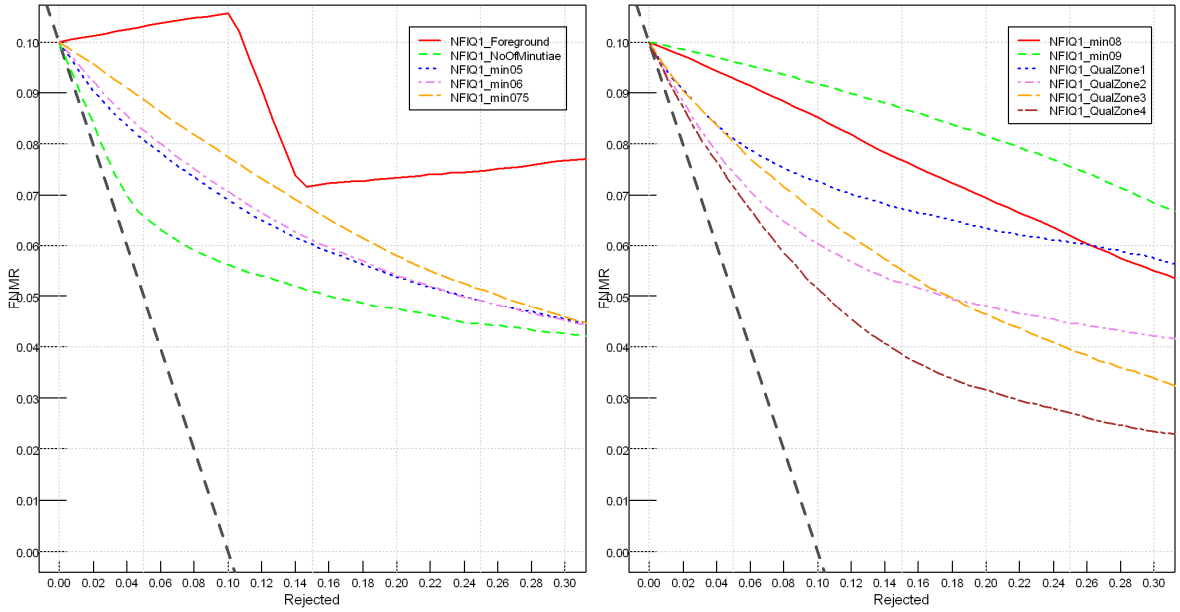

Figure 6: ERC of NFIQ 1 features at 10% FNMR for provider 28

4.2 Evaluation of the FingerJetFX Features

It turned out that some of the FingerJetFX features always returned the same value:

- The fingerprint quality is hard coded in the source code to the value 86.
- No minutiae with quality value between 0 and 0.4 were detected.

The spearman correlation matrix is shown below.

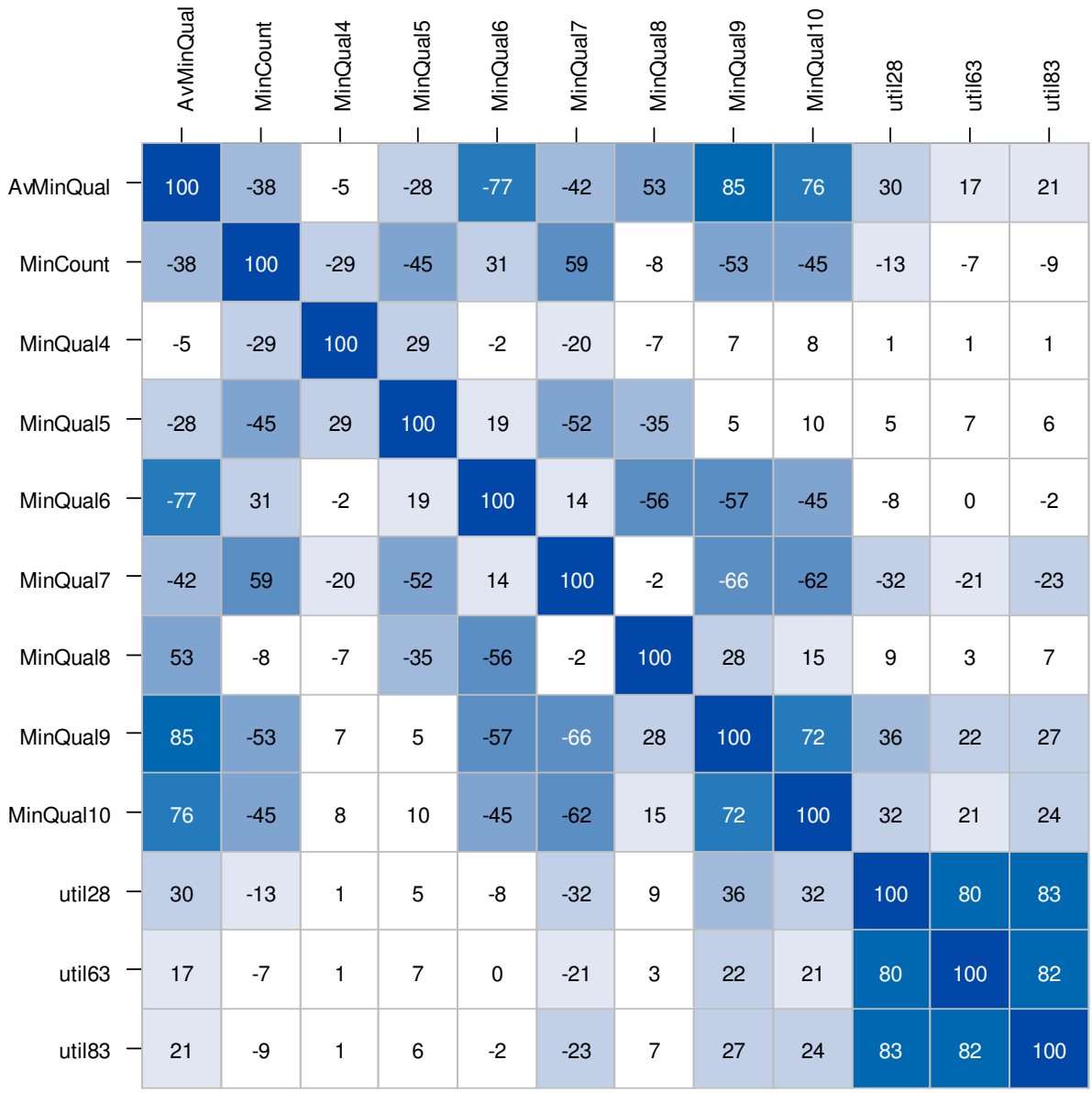

Table 4: Spearman correlation coefficients for NFIQ1 features

The highest correlation with utility was observed (in that order) for

1. Minutiae Quality 9
2. Minutiae Quality 10
3. Minutiae Quality 7
4. Average Minutiae Quality

Scatter plots of the features with provider 63 utility according to ISO 28784-1 [5] and density plots of the empirical feature distributions are shown in Appendix A.1.

4.2.1.1 ROC Curve Evaluation

The following table shows for the remaining FingerJetFX features, which selection criterion, i.e. choosing the impression with highest feature value or selecting the one with lowest feature value, results in better a ROC curve.

Feature	Abbr.	Criterion
AverageMinutiaeQuality	AMQ	lowest
MinutiaeCount	MinCount	lowest
MinutiaeQuality_4	MQ4	highest
MinutiaeQuality_5	MQ5	highest
MinutiaeQuality_6	MQ6	highest
MinutiaeQuality_7	MQ7	lowest
MinutiaeQuality_8	MQ8	lowest
MinutiaeQuality_9	MQ9	highest
MinutiaeQuality_10	MQ10	highest

Table 5: Optimal selecton criteria for ROC curves

For these criteria, the ROC curves are shown in Figures

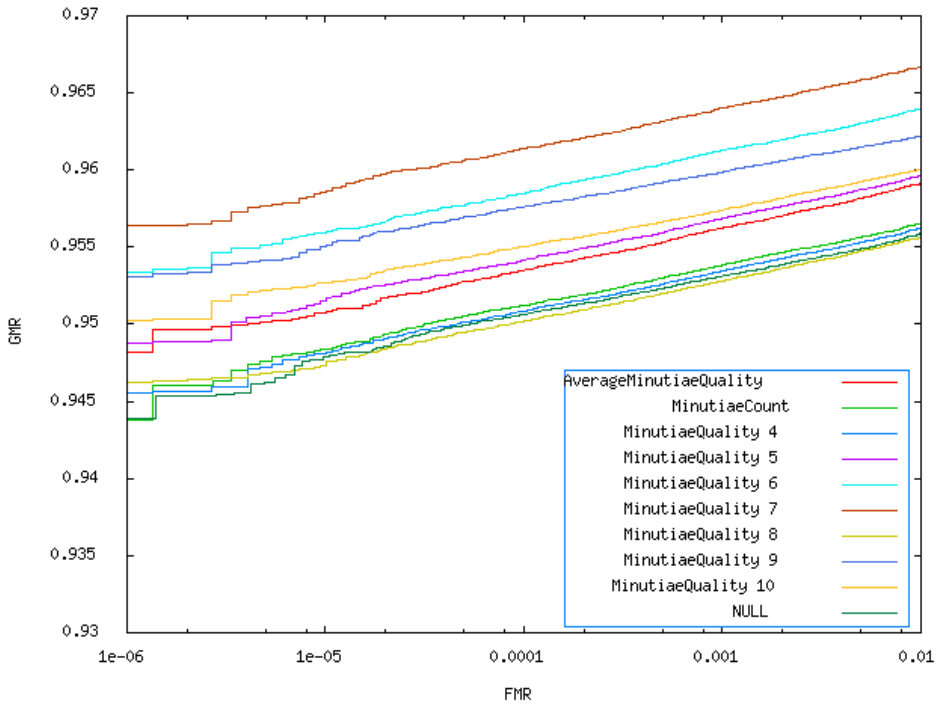

Figure 7: ROC curves of FingerJet FX features for provider 28

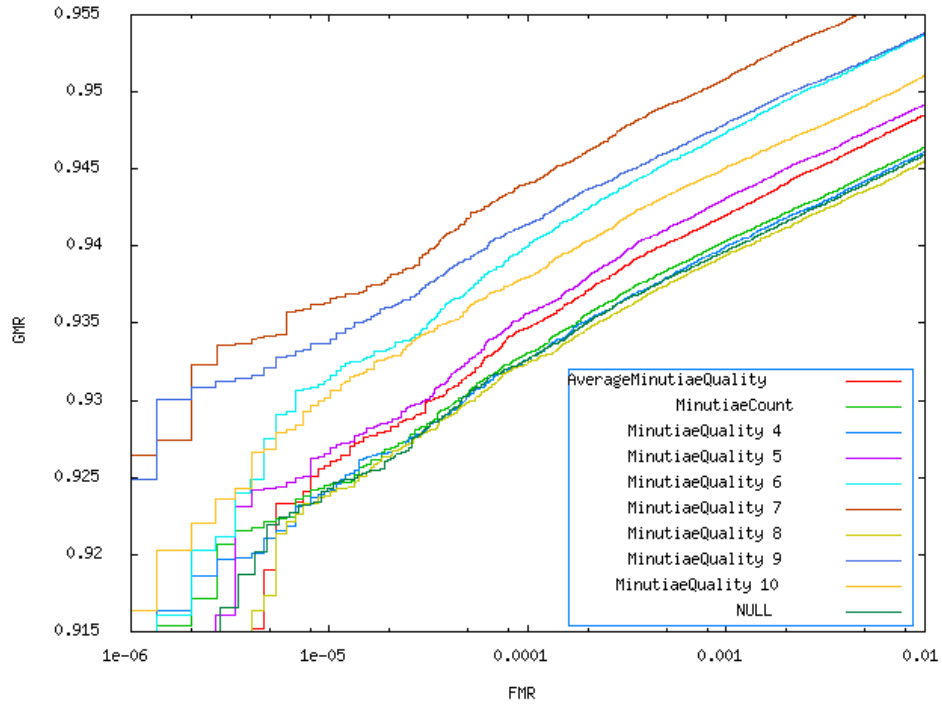

Figure 8: ROC curves of FingerJet FX features for provider 63

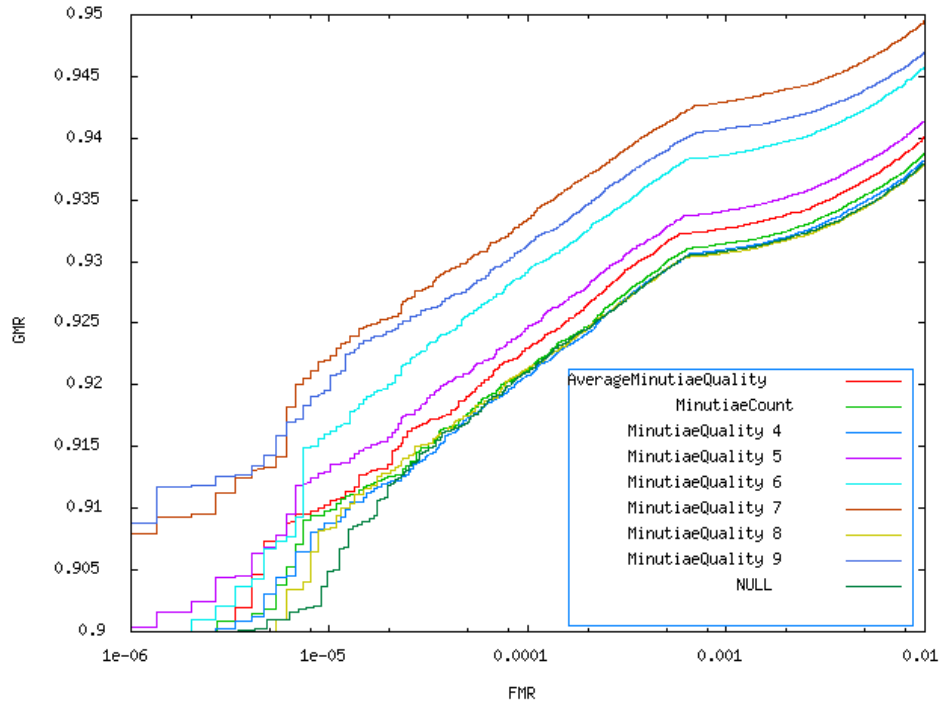

Figure 9: ROC curves of FingerJet FX features for provider 83

The following observations were made:

- Minutiae Quality 7 took ranked first for all providers.
- For provider 63 and 83, Minutiae Quality 9 and Minutiae Quality 6 took the second and third place, for provider 28 these ranks were exchanged.

- Consistently, Minutiae Count, Minutiae Quality 4, and Minutiae Quality 8 showed very poor performance.

4.2.1.2 ERC Evaluation

For the FingerJet FX features the following ERC curves were obtained for FNMR of 3% and 10%. Again, the dotted diagonal line from (0.1, 0) to (0, 0.1) for 10% FNMR and from (0.03,0) to (0.03,0) for 3% FNMR shows the ideal (and hypothetical) ERC in case of a perfect quality filtering, where scores are rejected according to their quality, starting with the lowest quality value.

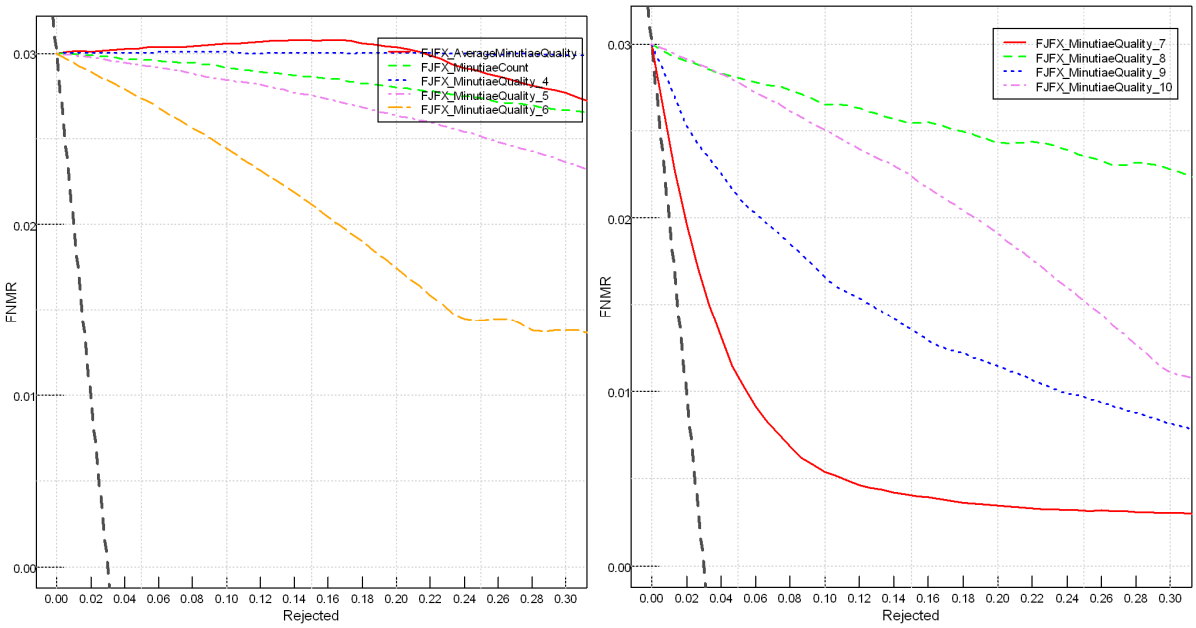

Figure 10: ERC of FingerJetFX features at 3% FNMR for provider 28

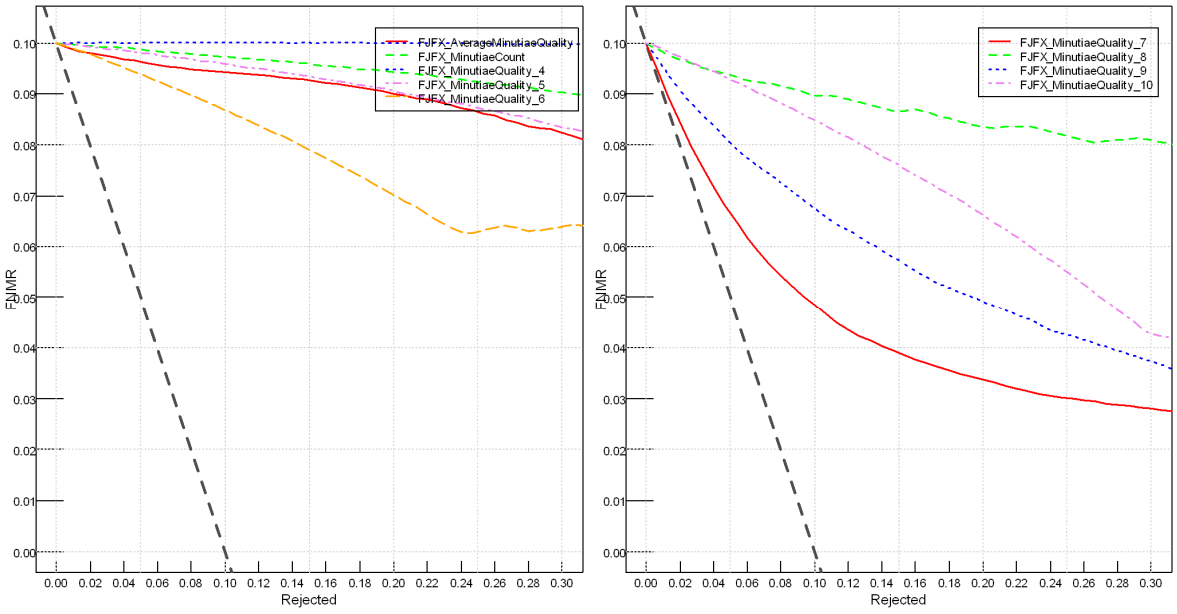

Figure 11: ERC of FingerJetFX features at 10% FNMR for provider 28

4.3 Evaluation of the Features Implemented by hda

For each of the features implemented by hda (see Section 2.3), 13 configurations were tested, resulting in 208 different feature instances. The following Table shows the configurations used.

	Config0	Config1	Config2	Config3	Config4	Config5	Config6	Config7	Config8	Config9	Config10	Config11	Config12
segmentBlocksizeValue	32	16	16	16	32	32	32	16	32	16	32	32	16
segmentTresholdValue	0.1	0.1	0.1	0.1	0.1	0.1	0.1	0.1	0.1	0.1	0.1	0.1	0.1
qualityBlocksizeValue	32	16	16	16	32	32	32	16	32	16	32	32	16
orientationFlowBorderValue	1	1	1	1	1	1	1	1	1	1	1	1	1
orientationFlowAngminValue	0	0	4	-4	0	4	-4	0	-4	0	4	0	-4
slantedBlocksizeValue	32,16	16,8	16,8	16,8	32,16	32,16	32,16	16,8	32,16	16,8	32,16	32,16	16,8
powerNradValue	30	20	30	40	20	30	20	40	30	30	30	40	40
powerNthetaValue	180	180	180	180	180	180	180	180	180	180	180	180	180
powerRminValue	25	20	25	30	20	25	20	30	25	30	20	30	30
powerNRmaxValue	84	64	84	104	64	64	104	84	64	64	104	64	64
gaborAnglesValue	8	4	6	8	4	6	8	6	4	8	6	5	5
gaborFreqValue	0.1	0.05	0.1	0.15	0.05	0.1	0.05	0.1	0.15	0.15	0.05	0.15	0.15
gaborSigmaValue	6	5	6	7	5	6	5	5	7	5	7	5	5
gaborShenTbValue	1	0.5	1	1.2	0.5	1	1.2	0.5	1.2	1.2	0.5	1.2	1.2
gaborShenTqValue	2	1.8	2	2.5	1.8	2	2.5	1.8	1.8	2.5	2.5	1.8	1.8

Table 6: Configurations used for feature computation

It turned out, that many configurations of a feature gave equivalent values, i.e. with spearman correlation of 1, or almost identical values resulting in a very high correlation. Furthermore, for all configurations, sigmaMuBlock and SigmaMuSigmaBlock gave almost equivalent values to MuMuSigmaBlock (correlation coefficient of -0.99). As a consequence, only 59 distinct instances (feature + configuration) remained.

Config	1	2	3	4	5	6	7	8	9	10	11	12
FDA		equiv1	equiv1	equiv0		equiv0	equiv1	equiv1	equiv0	equiv0	equiv0	equiv1
gabor				almost1								equiv11
GS				equiv1								equiv11
GSh		equiv0		equiv1		equiv3		equiv3			equiv9	equiv9
LCS		equiv1	equiv1			equiv0		equiv7	equiv0	equiv0	equiv0	equiv1
mu	Equiv0	equiv0	equiv0	equiv0	equiv0	equiv0	equiv0	equiv0	equiv0	equiv0	equiv0	equiv0
MMB		equiv1	equiv1	almost0	equiv0	equiv0	almost1	equiv7	equiv0	equiv0	equiv0	equiv1
MMSB		equiv1	equiv1	almost0	equiv0	equiv0	almost1	equiv7	equiv0	equiv0	equiv0	equiv1
MSB		equiv1	equiv1	almost0		equiv0	almost1	equiv7	equiv0	equiv0	equiv0	equiv1
OCL		equiv1	equiv1	equiv0	equiv0	equiv0	equiv1	equiv1	equiv0	equiv0	equiv0	equiv1
OF			equiv1	equiv0		equiv0	equiv1	equiv1	equiv6	equiv5	equiv0	equiv3
PS		equiv0	const0	equiv1	const0	const1	const0	const0	const0		const0	const0
RVU		equiv1	equiv1		equiv4	equiv0		equiv7	equiv0	equiv0	equiv0	equiv1
sigma	Equiv0	equiv0	equiv0	almost0	equiv0	equiv0	almost0	equiv7	equiv0	equiv0	equiv0	equiv0
SSB		equiv1	equiv1	almost0	equiv0	equiv0	almost1	equiv7	equiv0	equiv0	equiv0	equiv1

Table 7: Equivalent, almost identical or constant values of the feature configurations

Furthermore, we did not consider configurations of a feature that exhibited high correlations (greater than 0.875) with other configurations of the same feature. Of the remaining, i.e. the non-redundant, feature configurations, the following showed relatively (for the feature) good biometric performance in the ROC curve evaluation.

Config	0	1	2	5	7	9	10
FDA		x					
gabor	x						
GS				x		x	
GSh							x
LCS	x				X		
mu	x						
MMB	x	x					
MMSB	x						
MSB	x						
OCL	x						
OF			x				
PS	x						
RVU	x	x					
sigma	x						
SMB							
SSB		x					

Table 8: Non-redundant configurations giving relatively good performance for the feature

4.3.1.1 Correlation and scatter plots

For these feature, the correlation coefficients are given in the following table.

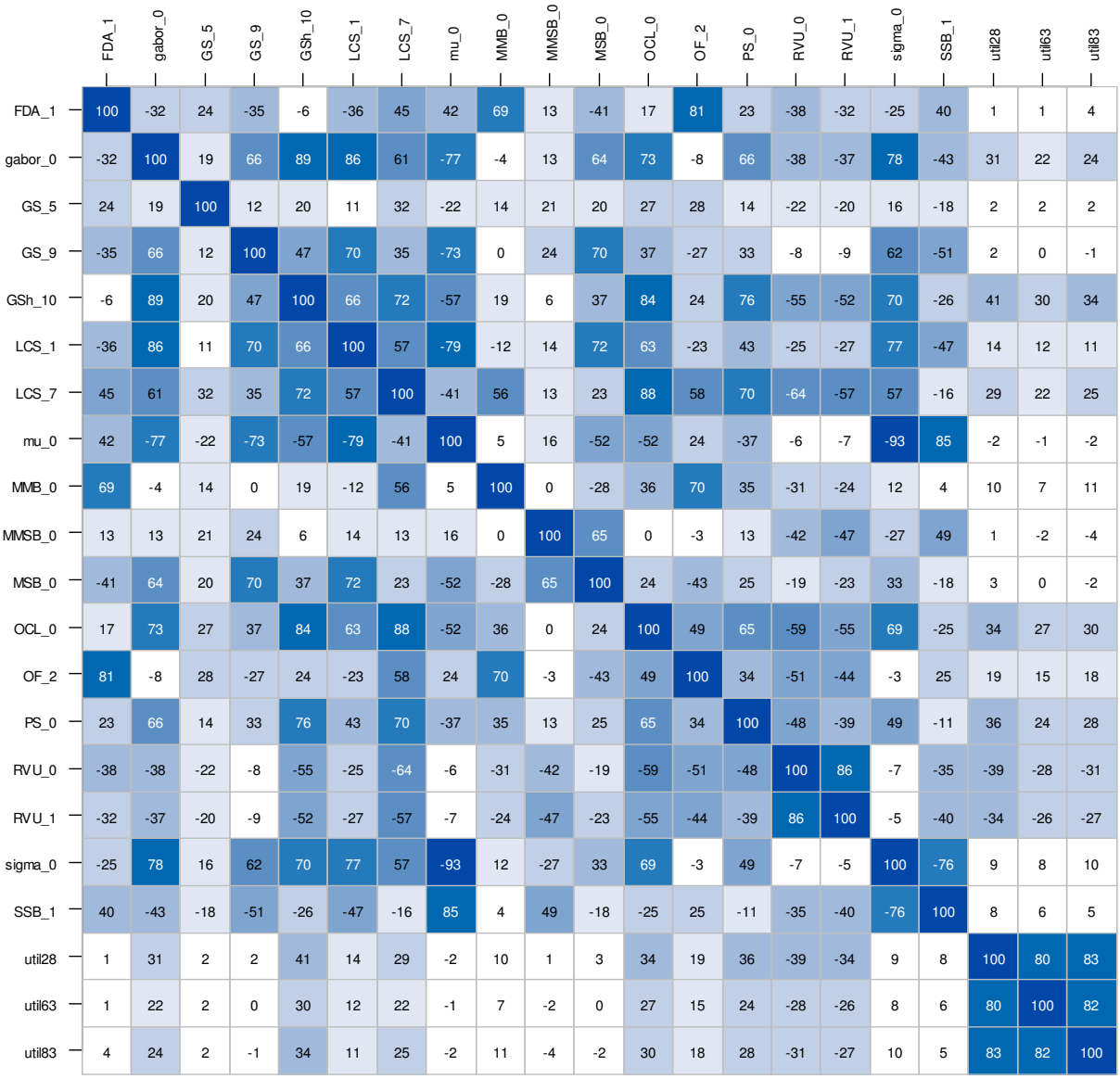

	FDA_1	gabor_0	GS_5	GS_9	GSh_10	LCS_1	LCS_7	mu_0	MMB_0	MMSB_0	MSB_0	OCL_0	OF_2	PS_0	RVU_0	RVU_1	sigma_0	SSB_1	util28	util63	util83
FDA_1	100	-32	24	-35	-6	-36	45	42	69	13	-41	17	81	23	-38	-32	-25	40	1	1	4
gabor_0	-32	100	19	66	89	86	61	-77	-4	13	64	73	-8	66	-38	-37	78	-43	31	22	24
GS_5	24	19	100	12	20	11	32	-22	14	21	20	27	28	14	-22	-20	16	-18	2	2	2
GS_9	-35	66	12	100	47	70	35	-73	0	24	70	37	-27	33	-8	-9	62	-51	2	0	-1
GSh_10	-6	89	20	47	100	66	72	-57	19	6	37	84	24	76	-55	-52	70	-26	41	30	34
LCS_1	-36	86	11	70	66	100	57	-79	-12	14	72	63	-23	43	-25	-27	77	-47	14	12	11
LCS_7	45	61	32	35	72	57	100	-41	56	13	23	88	58	70	-64	-57	57	-16	29	22	25
mu_0	42	-77	-22	-73	-57	-79	-41	100	5	16	-52	-52	24	-37	-6	-7	-93	85	-2	-1	-2
MMB_0	69	-4	14	0	19	-12	56	5	100	0	-28	36	70	35	-31	-24	12	4	10	7	11
MMSB_0	13	13	21	24	6	14	13	16	0	100	65	0	-3	13	-42	-47	-27	49	1	-2	-4
MSB_0	-41	64	20	70	37	72	23	-52	-28	65	100	24	-43	25	-19	-23	33	-18	3	0	-2
OCL_0	17	73	27	37	84	63	88	-52	36	0	24	100	49	65	-59	-55	69	-25	34	27	30
OF_2	81	-8	28	-27	24	-23	58	24	70	-3	-43	49	100	34	-51	-44	-3	25	19	15	18
PS_0	23	66	14	33	76	43	70	-37	35	13	25	65	34	100	-48	-39	49	-11	36	24	28
RVU_0	-38	-38	-22	-8	-55	-25	-64	-6	-31	-42	-19	-59	-51	-48	100	86	-7	-35	-39	-28	-31
RVU_1	-32	-37	-20	-9	-52	-27	-57	-7	-24	-47	-23	-55	-44	-39	86	100	-5	-40	-34	-26	-27
sigma_0	-25	78	16	62	70	77	57	-93	12	-27	33	69	-3	49	-7	-5	100	-76	9	8	10
SSB_1	40	-43	-18	-51	-26	-47	-16	85	4	49	-18	-25	25	-11	-35	-40	-76	100	8	6	5
util28	1	31	2	2	41	14	29	-2	10	1	3	34	19	36	-39	-34	9	8	100	80	83
util63	1	22	2	0	30	12	22	-1	7	-2	0	27	15	24	-28	-26	8	6	80	100	82
util83	4	24	2	-1	34	11	25	-2	11	-4	-2	30	18	28	-31	-27	10	5	83	82	100

Table 9: Spearman correlation coefficients for hda features

The highest correlation with utility was observed (in that order) for

1. Gabor Shen
2. Ridge Valley Uniformity (config 0)
3. Power Spectrum
4. Orientation Certainty Level
5. Ridge Valley Uniformity (config 1)
6. Local Clarity Score (config 7)

Scatter plots of the features with provider 63 utility according to ISO 28784-1 [5] and density plots of the empirical feature distributions are shown in Appendix A.1.

4.3.1.2 ROC Curve Evaluation

For some features, the optimal selection criterion, i.e. if choosing the impression with highest feature value or selecting the one with lowest feature value, results in better ROC curves, varied among the configurations. However, for the better performing configurations of each feature, the criterion was consistent. The following table shows the optimal selection criterion for the hda features.

Feature	Abbr.	Criterion
Frequency Domain Analysis	FDA	highest
Gabor	gabor	Highest
Gabor Segment 5	GS5	Lowest
Gabor Segment 9	GS9	Lowest
Gabor Shen	GSh	Highest
Local Clarity Score 1	LCS1	Highest
Local Clarity Score 7	LCS	Highest
Mu	mu	Highest
Mu Mu Block	MMB	Highest
Mu Mu Sigma Block	MMSB	Lowest
Mu Sigma Block	MSB	Lowest
Orientation Certainty Level	OCL	Highest
Orientation Flow	OF	Highest
Power Spectrum	PS	Highest
Ridge Valley Uniformity 0	RVU0	Lowest
Ridge Valley Uniformity 1	RVU1	Lowest
Sigma	sigma	Highest
Sigma Sigma Block	SSB	Highest

Table 10: Optimal selection criteria for hda features

The ROC curves of the best configurations are shown below. Where several configurations of a feature are included, they are indicated by the number following the feature name.

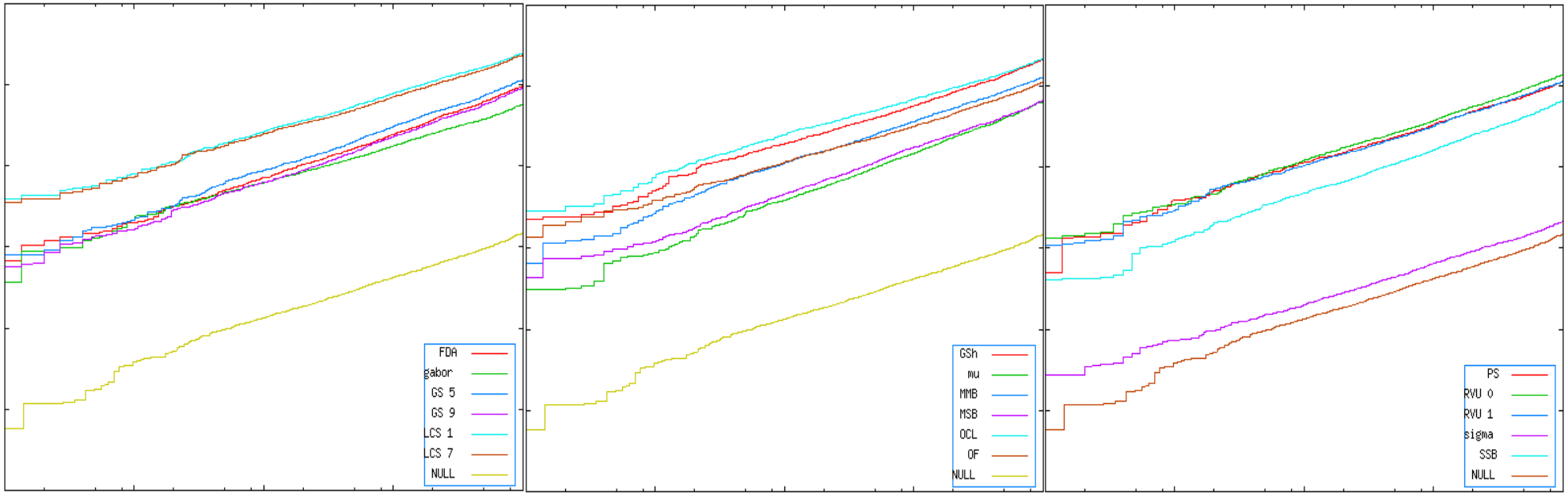

Figure 12: Provider 28 ROC curves for hda features

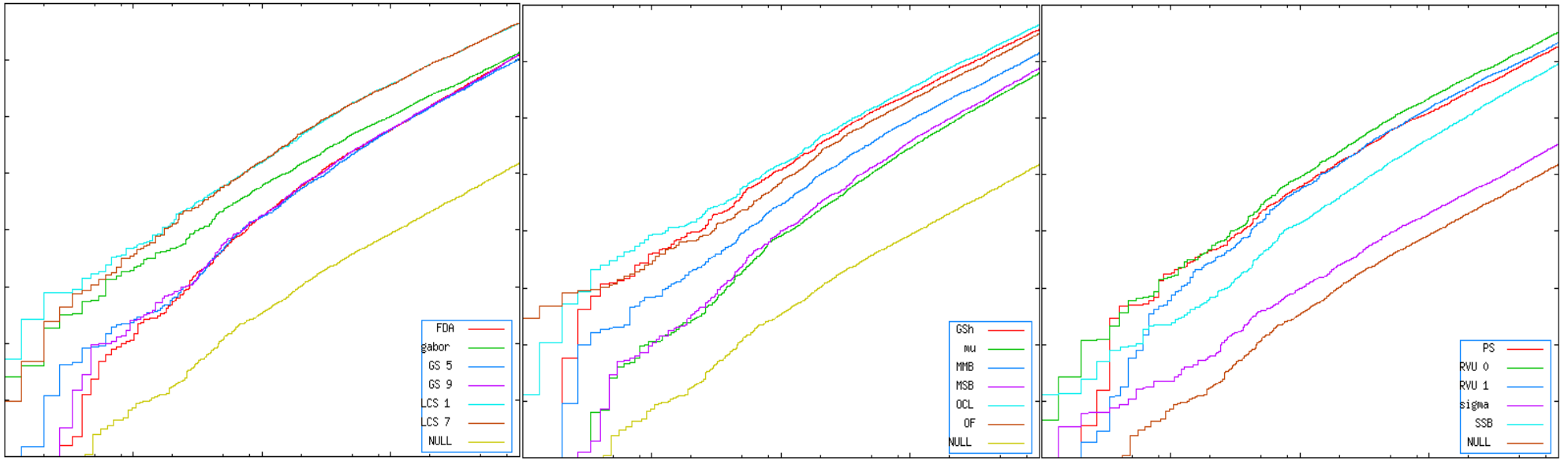

Figure 13: Provider 63 ROC curves for hda features

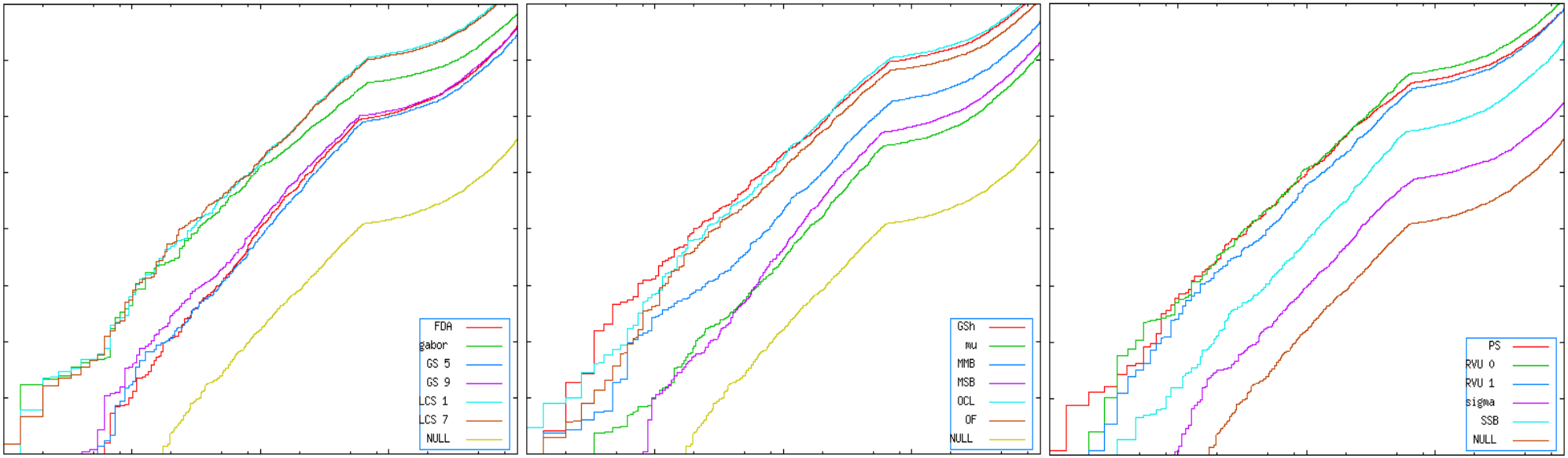

Figure 14: ROC curves for hda features for Provider 63 (top line) and provider 83

The best features are compared in the following ROC curve. Only the best configuration per feature is shown.

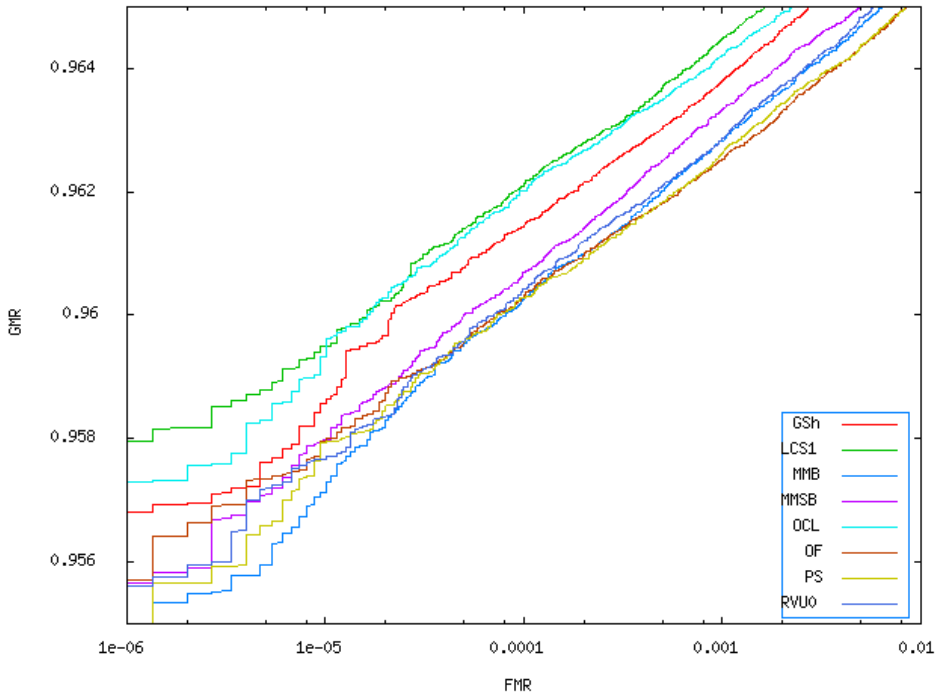

Figure 15: Provider 28 ROC curves of best had features

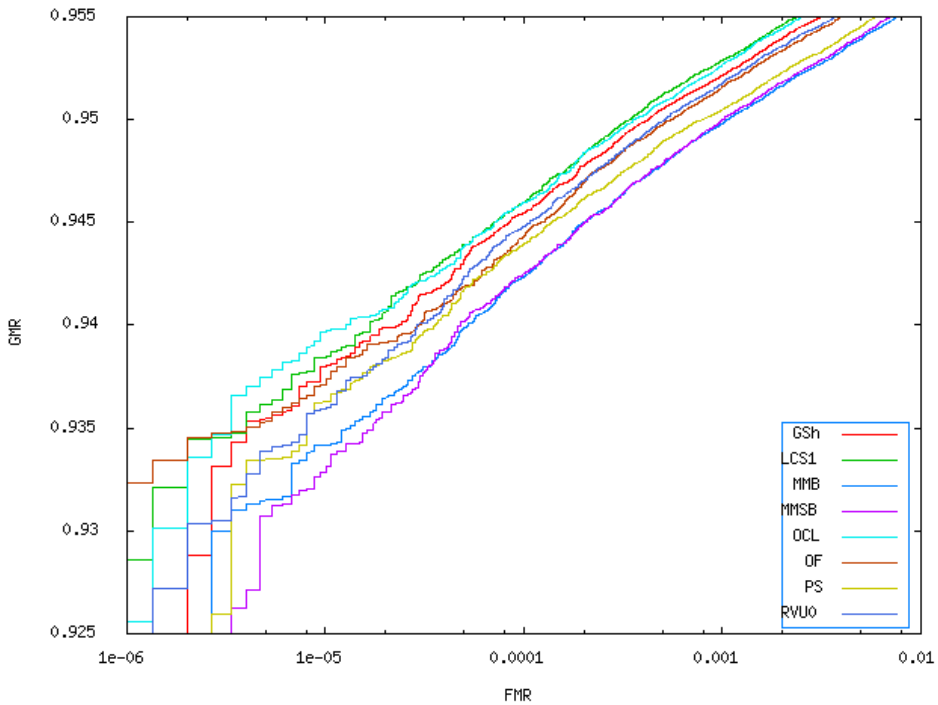

Figure 16: Provider 63 ROC curves of best features

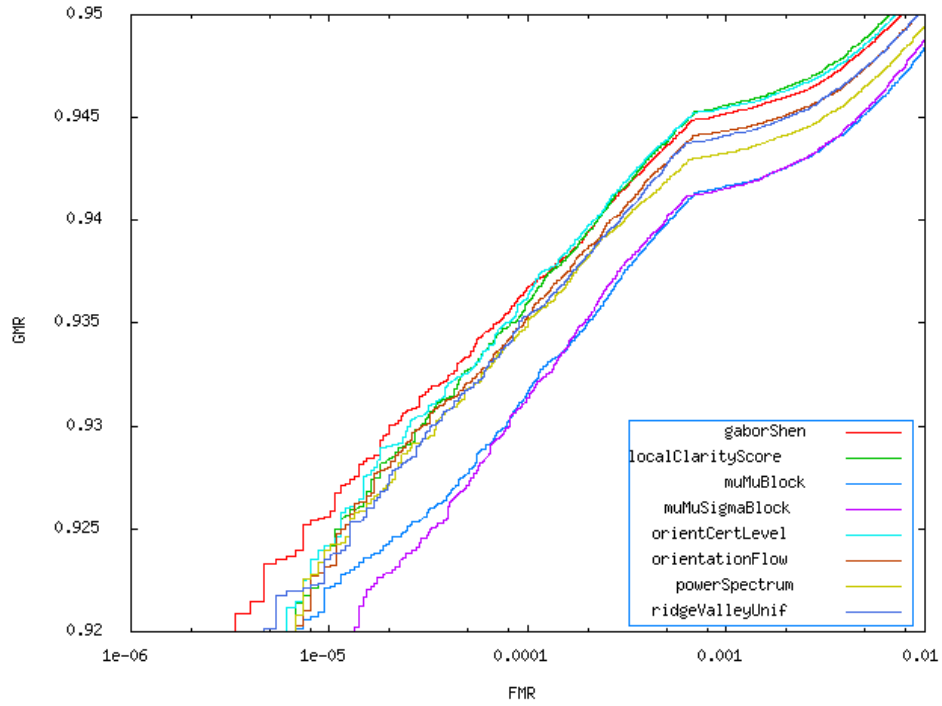

Figure 17: Provider 83 ROC curves of best features

The following observations were made on the ROC curves:

- For provider 28 and 63, Local Clarity Score and Orientation Certainty Level gave best performance, LCS being slightly better for provider 28.
- LCS was top performing for configurations 1 and 7. Although the values computed with these configurations have a spearman correlation coefficient of only 0.57, the scatter plot in Appendix A3 shows that for most fingerprints they are very close.
- For provider 28 and 63, Gabor Shen was clearly at the third rank.
- For provider 83, LCS and OCL were also top ranked but slightly beaten by Gabor Shen for FMR below 0.01%.
- For provider 28, Mu Mu Sigma Block was on rank four, while for rpoviders 63 nd 83, the fourth rank was shared by Orientation Flow and Ridge Vally Uniformity.
- For provider 28, the fifth rank was shared by Mu Mu Block and Ridge Valley Uniformity, while for providers 63 and 83, it was taken by Power Spectrum.
- For all providers, Sigma gave poor performance.

Overall, the results of the ROC curve evaluation were quite consistent among the providers. The top ranking had features are shown in the following Table

Provider 28	**Provider 63**	**Provider 83**
Local Clarity Score (1&7)	Local Clarity Score (1&7) Orientation Certainty Level	Local Clarity Score (1&7) Orientation Certainty Level Gabor Shen (low FMR)
Orientation Certainty Level		
Gabor Shen	Gabor Shen	
Mu Mu Sigma Block	Ridge Valley Uniformity 0 Orientation Flow	Ridge Valley Uniformity 0 Orientation Flow
Mu Mu Block Ridge Valley Uniformity 0	Power Spectrum	Power Spectrum
Power Spectrum Orientation Flow	Mu Mu Block Mu Mu Sigma Block	Mu Mu Block Mu Mu Sigma Block

Table 11: Top ranks of ROC evaluation for hda features

4.3.1.3 ERC Evaluation

For the features developed by hda the following ERC curves at 3% FNMR and 10% FNMR were obtained. Again, the dotted diagonal line from (0.1, 0) to (0, 0.1) for 10% FNMR and from (0.03, 0) to (0, 0.03) for 3% FNMR shows the ideal (and hypothetical) ERC in case of a perfect quality filtering, where scores are rejected according to their quality, starting with the lowest quality value.

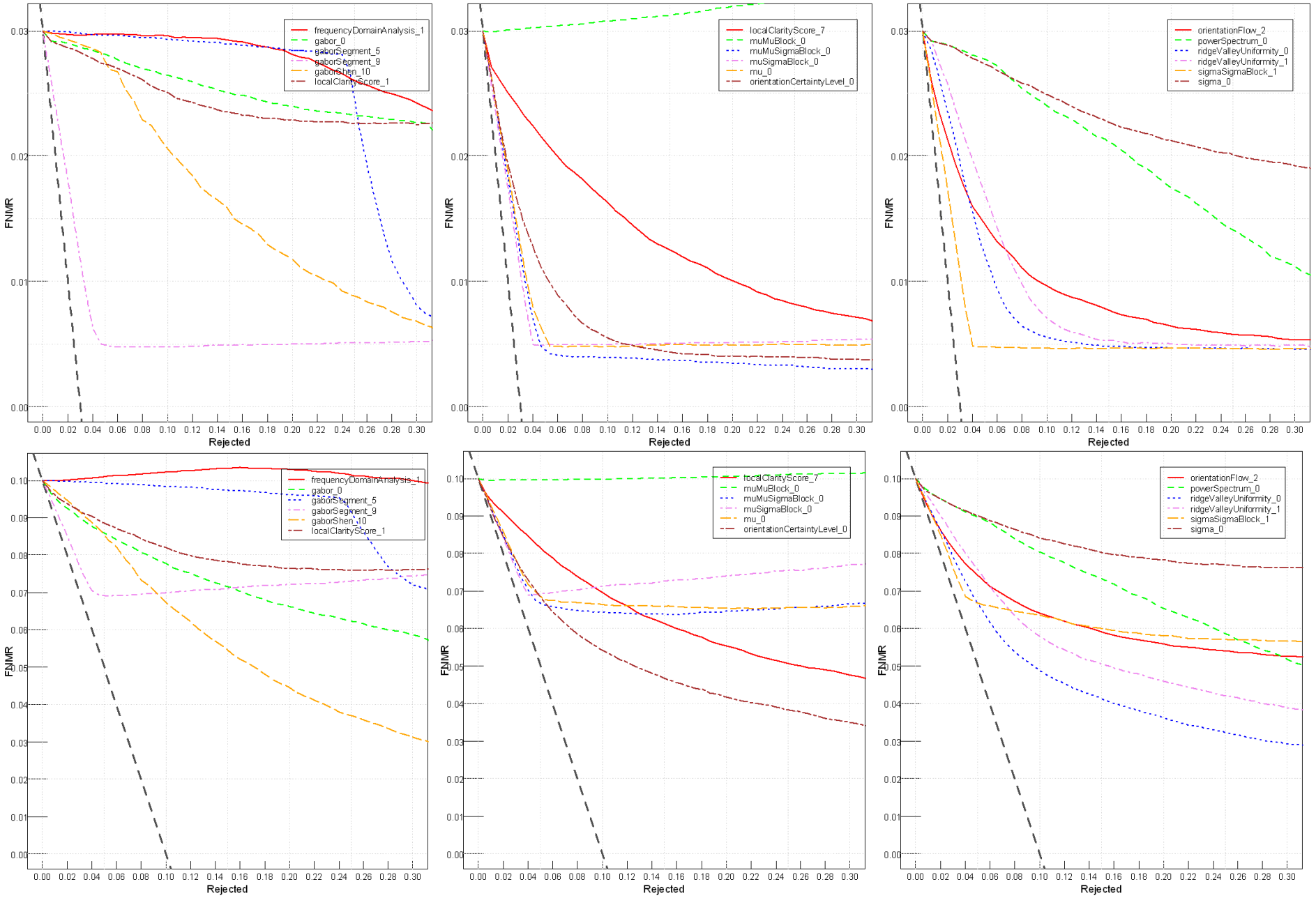

Figure 18: ERC for hda features at 3% FNMR (top line) and 10% FNMR (bottom line) for provider 28

It turned out than some features, namely Gabor Segment 9, Mu Mu Sigma Block, Mu Sigma Block, Mu and Sigma Sigma Block, resulted in similar ERC where the FNMR rapidly decreases for the first 2.5 -3% but from that point on shows only moderate reduction. This phenomenon can be explained as follows: approximately 4-5% of the genuine comparisons for provider 28 give extremely low comparison scores, which is clearly visible in the density function plot below.

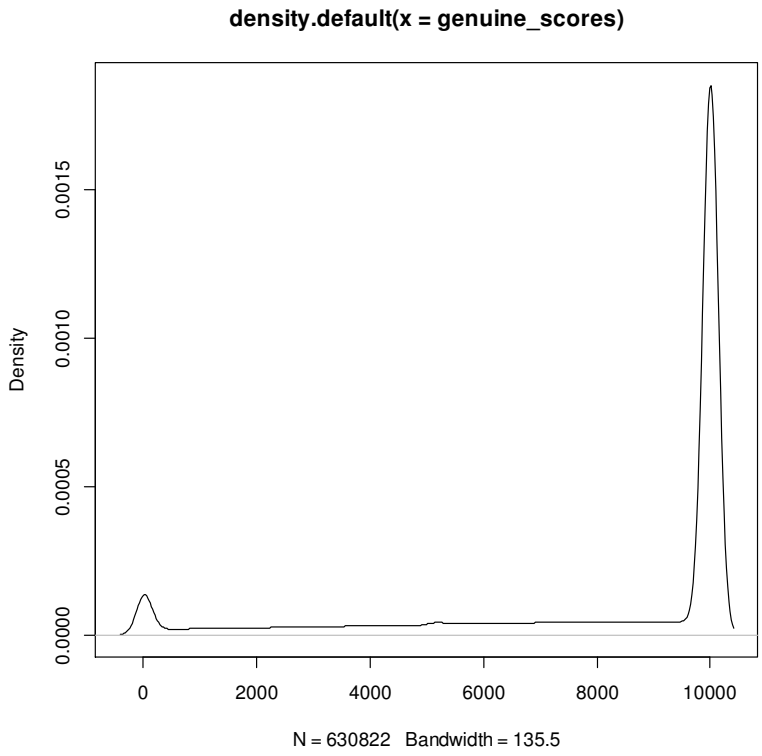

Figure 19: Density function of genuine scores for provider 28

Approximately 3% of these “bad genuine scores” seem to be caused by fingerprints with extreme (highest or lowest) feature values for these features, which implies that filtering by these feature values filters very well these 3% of the bad genuine scores. At least for Mu Mu Sigma Block, Mu Sigma Block, Mu and Sigma Sigma Block, this explanation is supported by the scatter plots of genuine scores (for provider 28) and minimum (or maximum, depending on the sign of correlation between feature values and genuine scores) quality values of sample and probe fingerprint: for each of these features, in the very bottom of the scatter plot there is a strong accumulation or a wedge either in the very left (in case where the genuine scores correlate positively with feature values) or in the very right (in case of negative correlation).

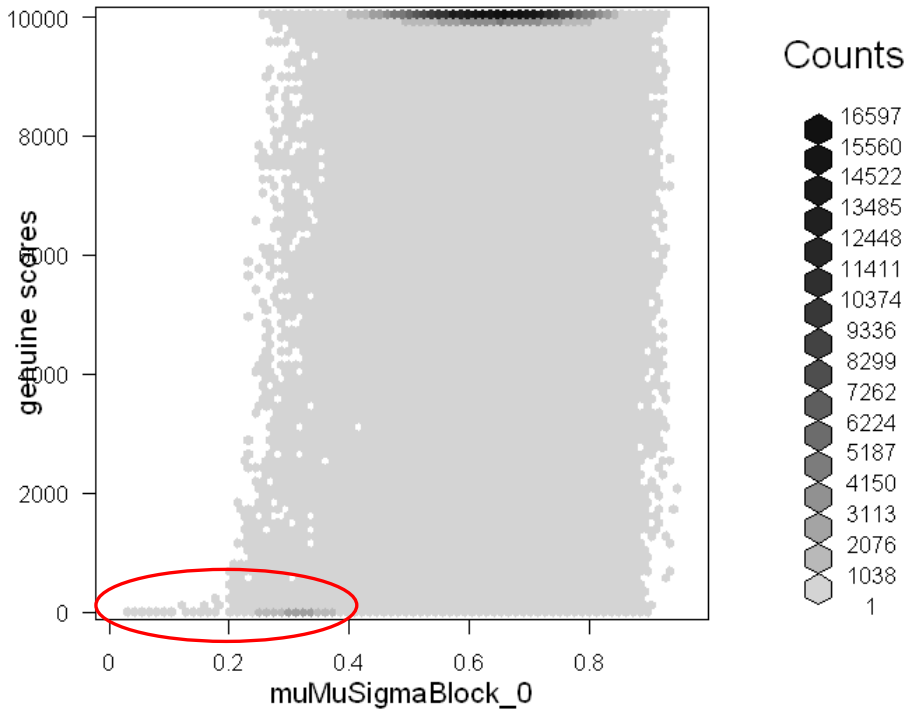

Figure 20: Scatter plot of genuine scores and Mu Mu Sigma Block

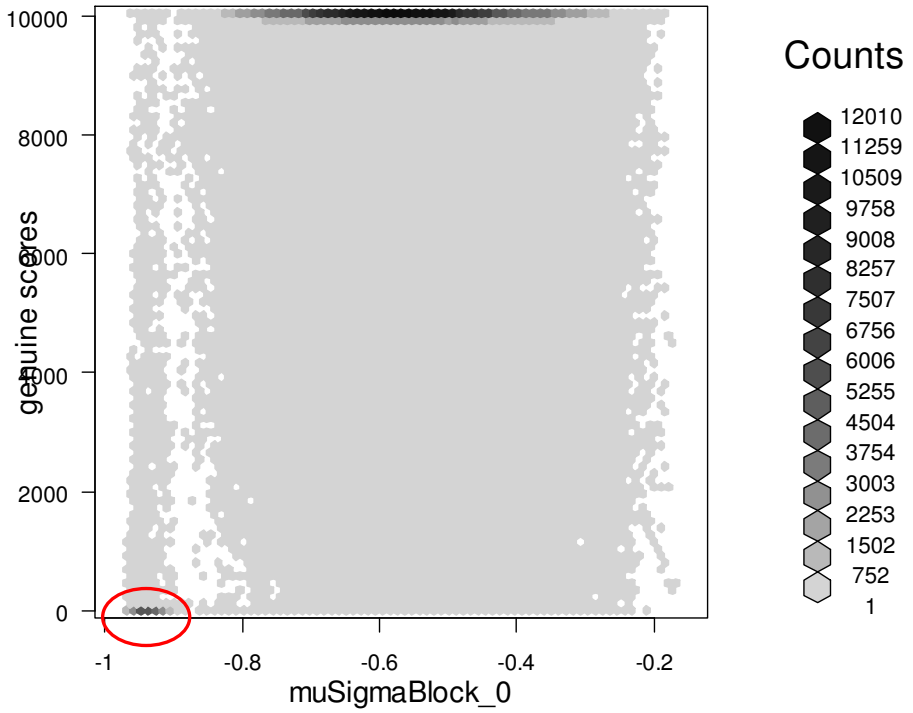

Figure 21: Scatter plot of genuine scores and Mu Sigma Block

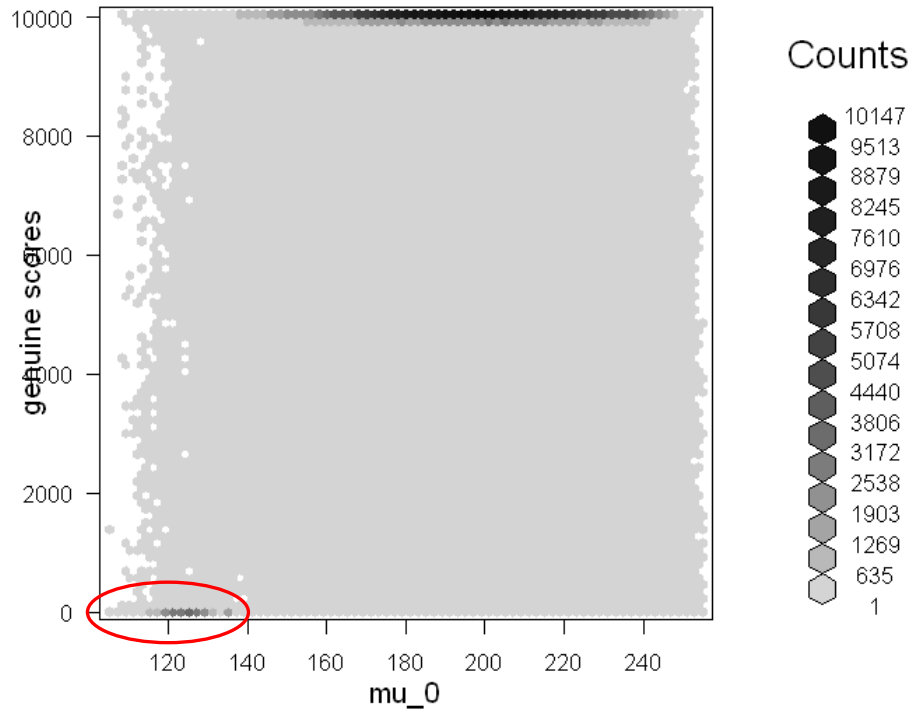

Figure 22: Scatter plot of genuine scores and Mu

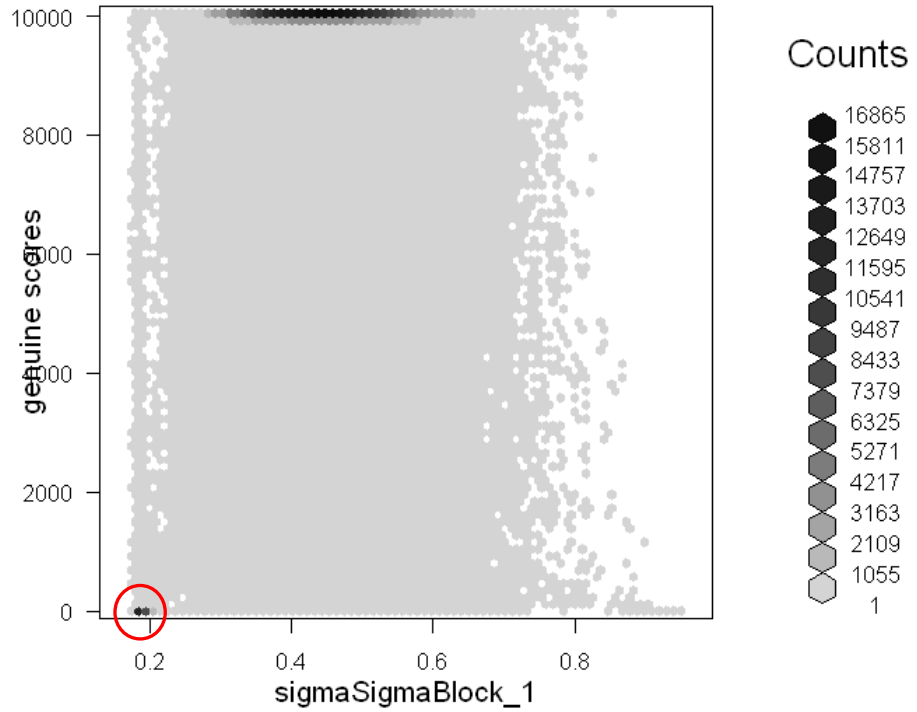

Figure 23: Scatter plot of genuine scores and Sigma Sigma Block

Furthermore, the ERC indicate that the filtering effect by these features is quite similar. This hypothesis is supported by the well-separated accumulations in the corners of the scatter plots among these features, showing that the subsets of genuine scores filtered by these features strongly overlap. This effect is particularly strong for Mu Sigma Block and Sigma Sigma Block.

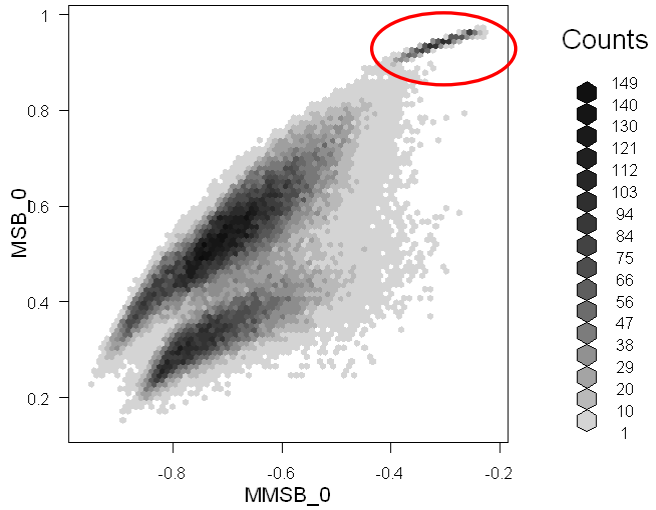

Figure 24: Scatter plot of Mu Sigma Block and Mu Mu Sigma Block

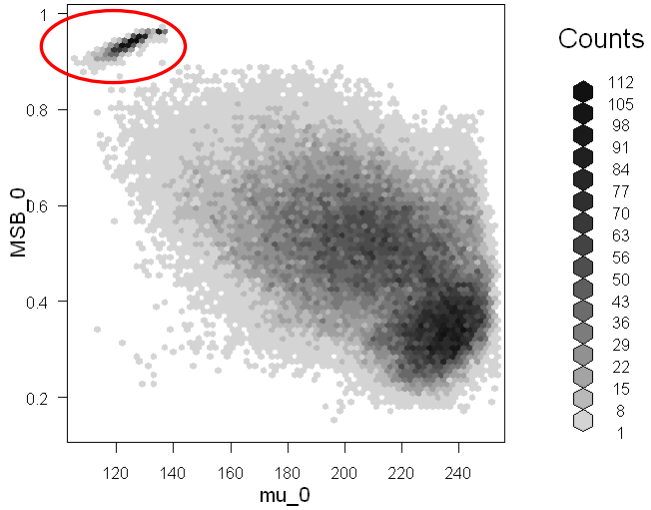

Figure 25: Scatter plot of Mu Sigma Block and Mu

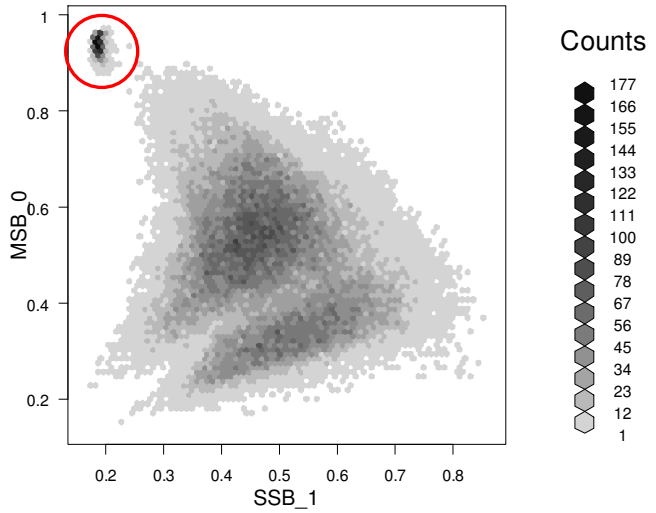

Figure 26: Scatter plot of Mu Sigma Block and Sigma Sigma Block

Due to the strong initial reduction of the FNMR down to 1% in the ERC for 3% FNMR, the features Gabor Segment 9, Mu Mu Sigma Block, Mu Sigma Block, Mu

and Sigma Sigma Block resulted in the lowest error rates up to 30% rejection rate. For this reason these features were top among the best in the ERC at 3% FNMR while only being mediocre performers in the ERC at 10% FNMR and rejection rate greater than 15%. This phenomenon resulted in different rankings for 3% FNMR and 10% FNMR.

FNMR = 3%	**FNMR = 10%**
Mu Mu Sigma Block	Ridge Valley Uniformity 0
Gabor Segment (config 9) Mu Mu Sigma Block Mu Mu Sigma Block Sigma Sigma Block	Orientation Certainty Level
	Gabor Shen
	Orientation Flow Local Clarity Score 7
Ridge Valley Uniformity 0 Orientation Certainty Level	Power Spectrum Gabor
Ridge Valley Uniformity 1	Ridge Valley Uniformity 1

Table 12: Top ranks of ERC evaluation for hda features

4.4 Overall Comparison

4.4.1 Correlation

The following Table shows the spearman correlation coefficients for the hda features with the top performing features of NFIQ1 (including Foreground) and FingerJet FX.

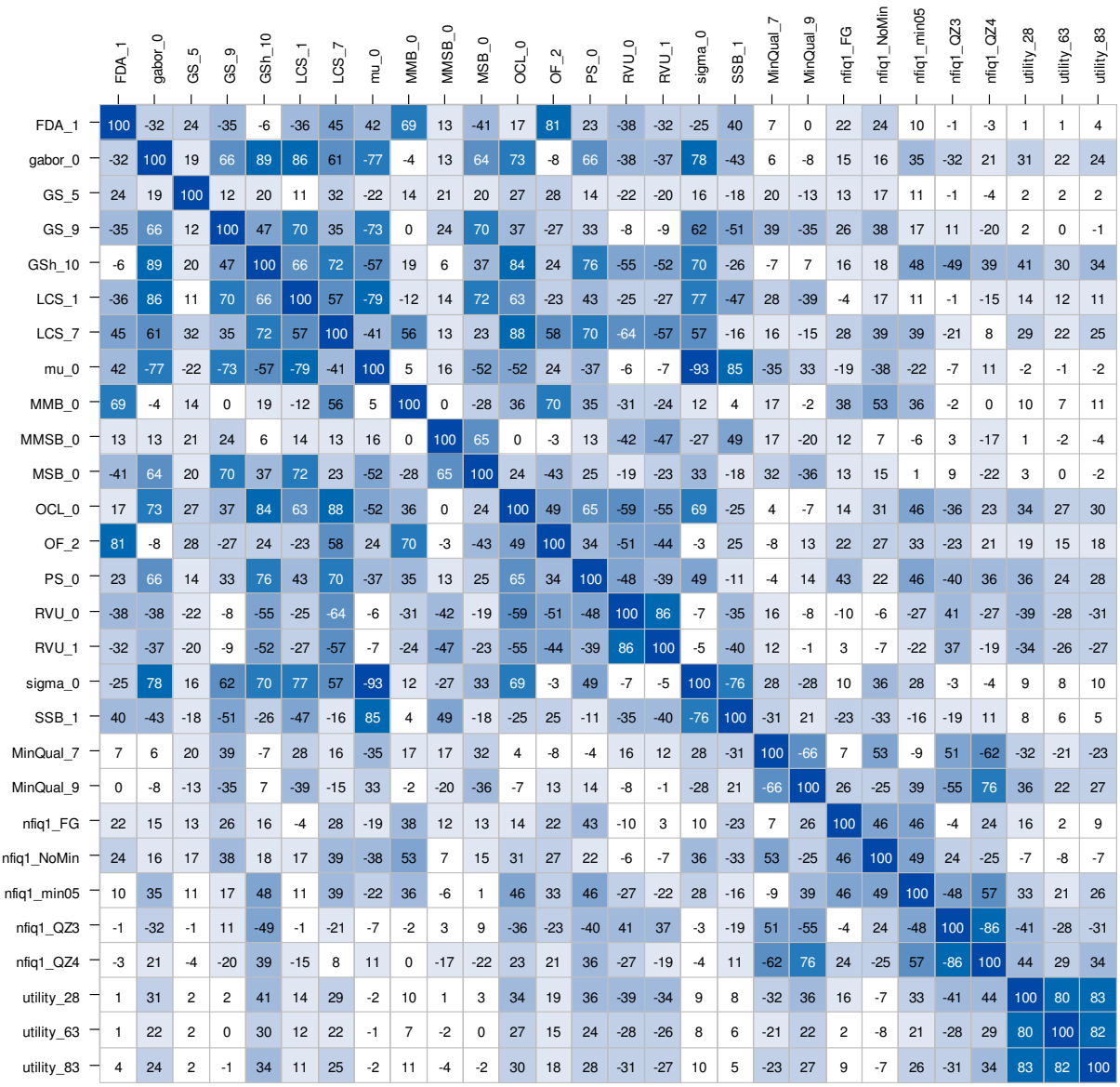

	FDA_1	gabor_0	GS_5	GS_9	GSh_10	LCS_1	LCS_7	mu_0	MMB_0	MMSB_0	MSB_0	OCL_0	OF_2	PS_0	RVU_0	RVU_1	sigma_0	SSB_1	MinQual_7	MinQual_9	nfiq1_FG	nfiq1_NoMin	nfiq1_min05	nfiq1_QZ3	nfiq1_QZ4	utility_28	utility_63	utility_83
FDA_1	100	-32	24	-35	-6	-36	45	42	69	13	-41	17	81	23	-38	-32	-25	40	7	0	22	24	10	-1	-3	1	1	4
gabor_0	-32	100	19	66	89	86	61	-77	-4	13	64	73	-8	66	-38	-37	78	-43	6	-8	15	16	35	-32	21	31	22	24
GS_5	24	19	100	12	20	11	32	-22	14	21	20	27	28	14	-22	-20	16	-18	20	-13	13	17	11	-1	-4	2	2	2
GS_9	-35	66	12	100	47	70	35	-73	0	24	70	37	-27	33	-8	-9	62	-51	39	-35	26	38	17	11	-20	2	0	-1
GSh_10	-6	89	20	47	100	66	72	-57	19	6	37	84	24	76	-55	-52	70	-26	-7	7	16	18	48	-49	39	41	30	34
LCS_1	-36	86	11	70	66	100	57	-79	-12	14	72	63	-23	43	-25	-27	77	-47	28	-39	-4	17	11	-1	-15	14	12	11
LCS_7	45	61	32	35	72	57	100	-41	56	13	23	88	58	70	-64	-57	57	-16	16	-15	28	39	39	-21	8	29	22	25
mu_0	42	-77	-22	-73	-57	-79	-41	100	5	16	-52	-52	24	-37	-6	-7	-93	85	-35	33	-19	-38	-22	-7	11	-2	-1	-2
MMB_0	69	-4	14	0	19	-12	56	5	100	0	-28	36	70	35	-31	-24	12	4	17	-2	38	53	36	-2	0	10	7	11
MMSB_0	13	13	21	24	6	14	13	16	0	100	65	0	-3	13	-42	-47	-27	49	17	-20	12	7	-6	3	-17	1	-2	-4
MSB_0	-41	64	20	70	37	72	23	-52	-28	65	100	24	-43	25	-19	-23	33	-18	32	-36	13	15	1	9	-22	3	0	-2
OCL_0	17	73	27	37	84	63	88	-52	36	0	24	100	49	65	-59	-55	69	-25	4	-7	14	31	46	-36	23	34	27	30
OF_2	81	-8	28	-27	24	-23	58	24	70	-3	-43	49	100	34	-51	-44	-3	25	-8	13	22	27	33	-23	21	19	15	18
PS_0	23	66	14	33	76	43	70	-37	35	13	25	65	34	100	-48	-39	49	-11	-4	14	43	22	46	-40	36	36	24	28
RVU_0	-38	-38	-22	-8	-55	-25	-64	-6	-31	-42	-19	-59	-51	-48	100	86	-7	-35	16	-8	-10	-6	-27	41	-27	-39	-28	-31
RVU_1	-32	-37	-20	-9	-52	-27	-57	-7	-24	-47	-23	-55	-44	-39	86	100	-5	-40	12	-1	3	-7	-22	37	-19	-34	-26	-27
sigma_0	-25	78	16	62	70	77	57	-93	12	-27	33	69	-3	49	-7	-5	100	-76	28	-28	10	36	28	-3	-4	9	8	10
SSB_1	40	-43	-18	-51	-26	-47	-16	85	4	49	-18	-25	25	-11	-35	-40	-76	100	-31	21	-23	-33	-16	-19	11	8	6	5
MinQual_7	7	6	20	39	-7	28	16	-35	17	17	32	4	-8	-4	16	12	28	-31	100	-66	7	53	-9	51	-62	-32	-21	-23
MinQual_9	0	-8	-13	-35	7	-39	-15	33	-2	-20	-36	-7	13	14	-8	-1	-28	21	-66	100	26	-25	39	-55	76	36	22	27
nfiq1_FG	22	15	13	26	16	-4	28	-19	38	12	13	14	22	43	-10	3	10	-23	7	26	100	46	46	-4	24	16	2	9
nfiq1_NoMin	24	16	17	38	18	17	39	-38	53	7	15	31	27	22	-6	-7	36	-33	53	-25	46	100	49	24	-25	-7	-8	-7
nfiq1_min05	10	35	11	17	48	11	39	-22	36	-6	1	46	33	46	-27	-22	28	-16	-9	39	46	49	100	-48	57	33	21	26
nfiq1_QZ3	-1	-32	-1	11	-49	-1	-21	-7	-2	3	9	-36	-23	-40	41	37	-3	-19	51	-55	-4	24	-48	100	-86	-41	-28	-31
nfiq1_QZ4	-3	21	-4	-20	39	-15	8	11	0	-17	-22	23	21	36	-27	-19	-4	11	-62	76	24	-25	57	-86	100	44	29	34
utility_28	1	31	2	2	41	14	29	-2	10	1	3	34	19	36	-39	-34	9	8	-32	36	16	-7	33	-41	44	100	80	83
utility_63	1	22	2	0	30	12	22	-1	7	-2	0	27	15	24	-28	-26	8	6	-21	22	2	-8	21	-28	29	80	100	82
utility_83	4	24	2	-1	34	11	25	-2	11	-4	-2	30	18	28	-31	-27	10	5	-23	27	9	-7	26	-31	34	83	82	100

Table 13: Spearman correlation coefficients of best performing features

An interesting observation is that high correlations (> 0.5) occur among the features implemented by hda as well as among FJFX and NFIQ1 features, but not between these two groups. This indicates that features from these two groups may well complement each other with respect to information content.

4.4.2 ROC Curve Evaluation

The following figures show the ROC curves of the top performing features.

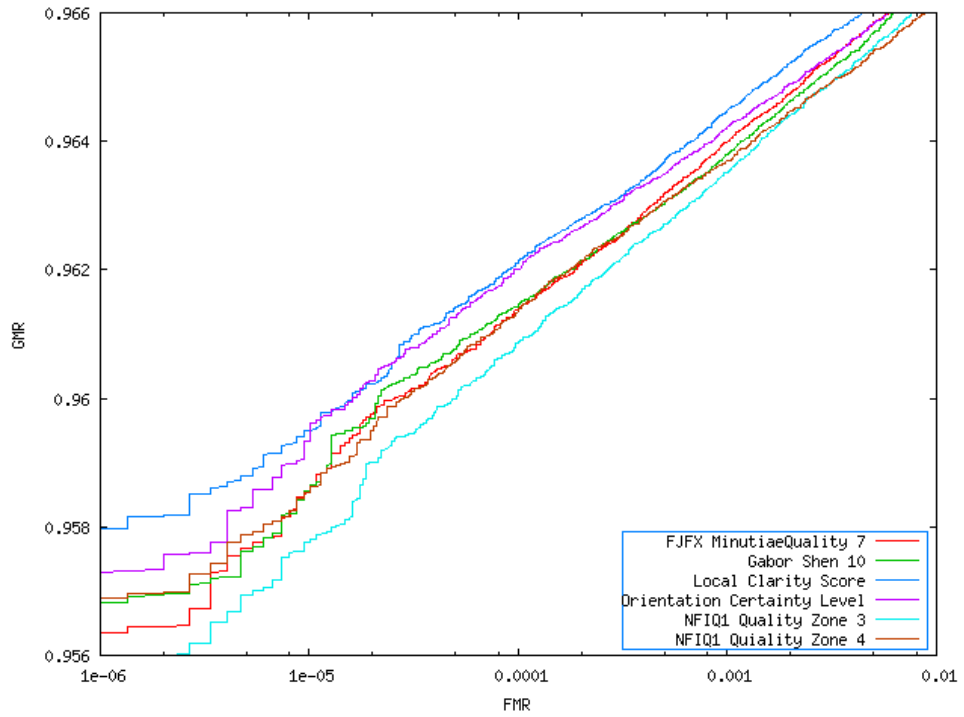

Figure 27: Provider 28 ROC curves of top performing features

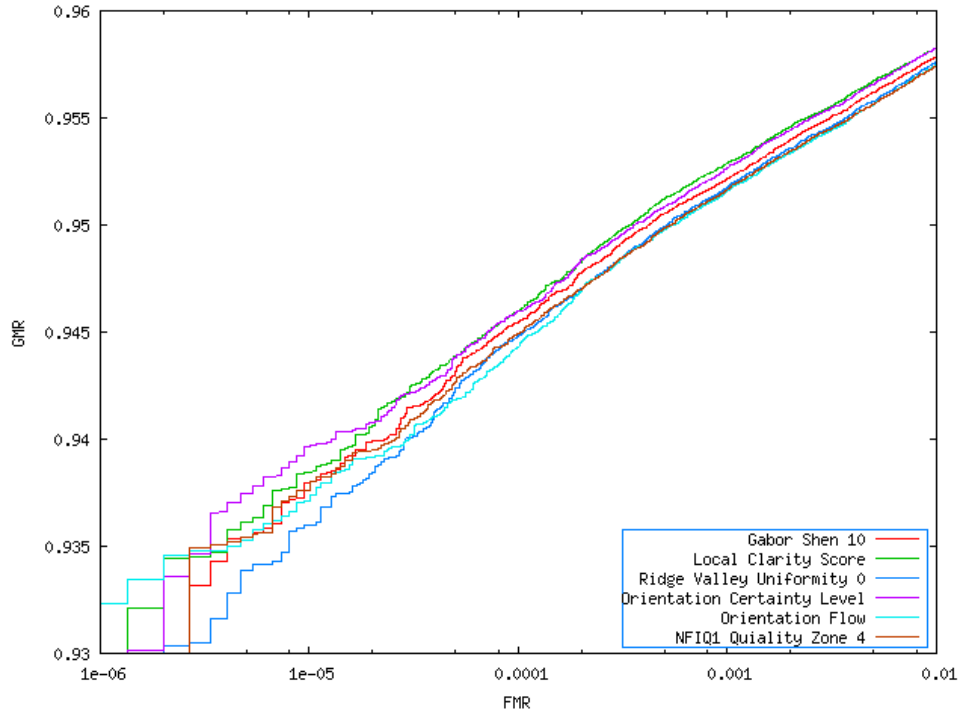

Figure 28: Provider 63 ROC curves of top performing features

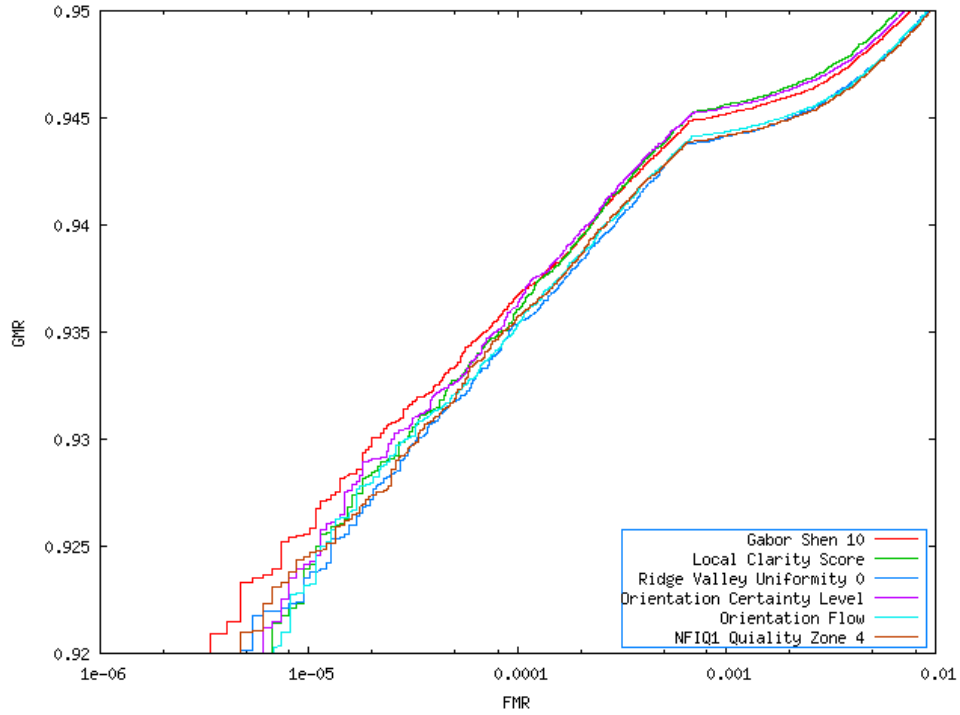

Figure 29: Provider 83 ROC curves of top performing features

Following these top performers we found the following features giving next best results.

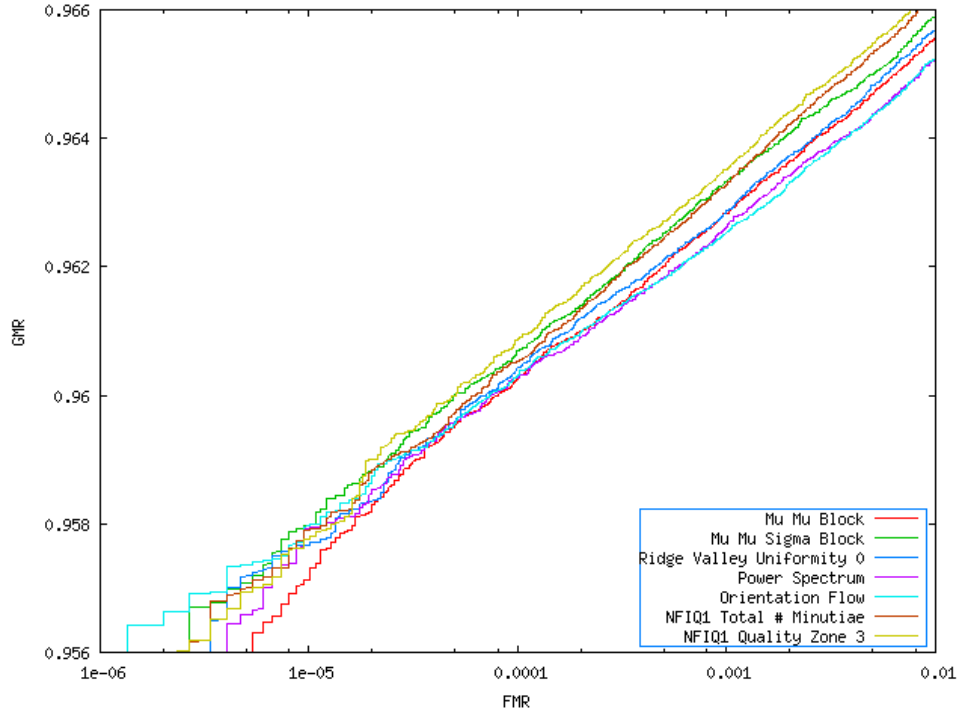

Figure 30: Provider 28 ROC curves of next best performing features

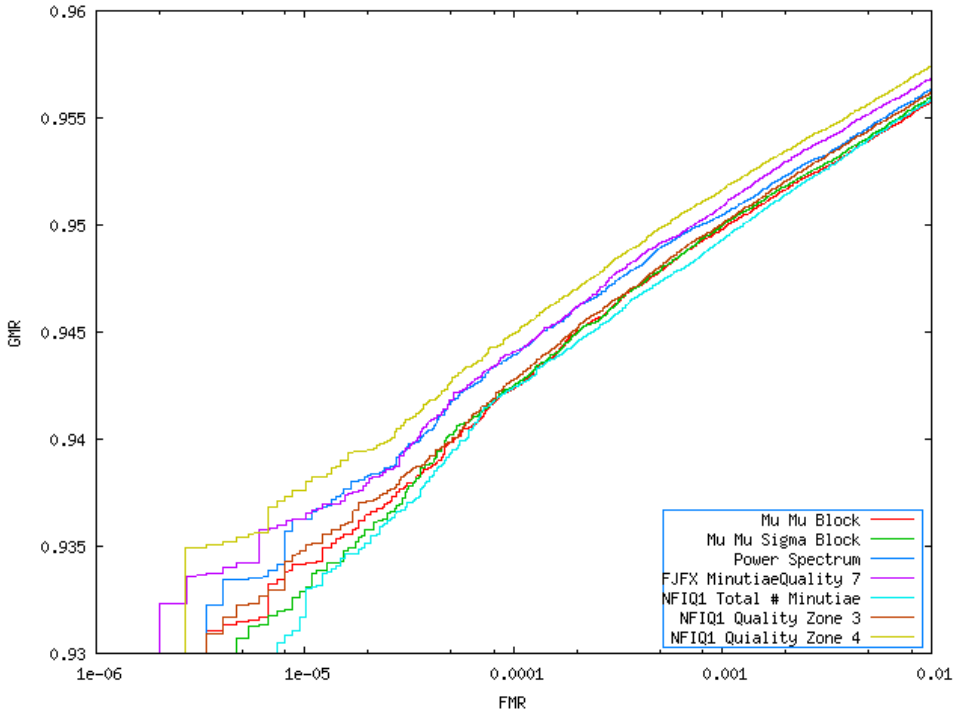

Figure 31: Provider 63 ROC curves of next best performing features

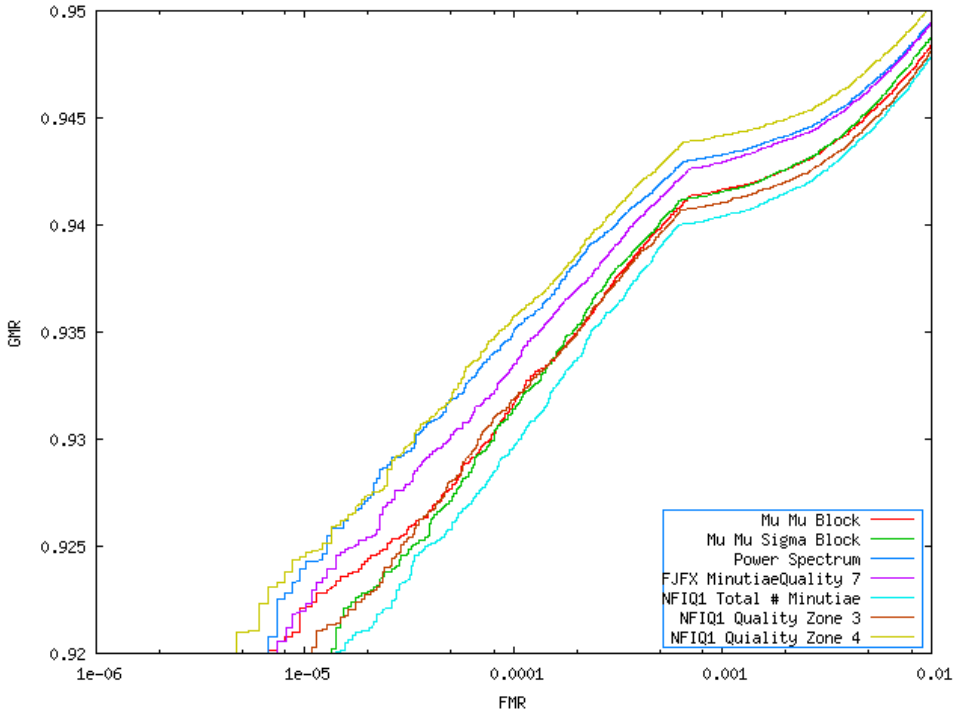

Figure 32: Provider 83 ROC curves of next best performing features

4.4.3 ERC evaluation

The following ERC curves show the best performing features at FNMR of 3% and FNMR at 10%.

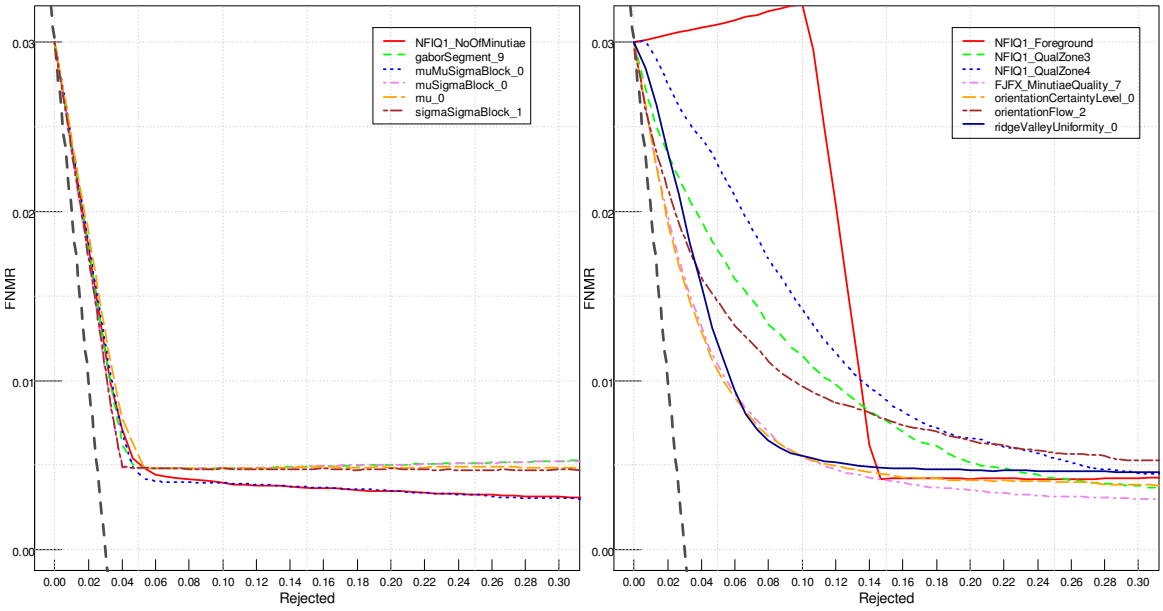

Figure 33: Best features in ERC at 3% FNMR for provider 28

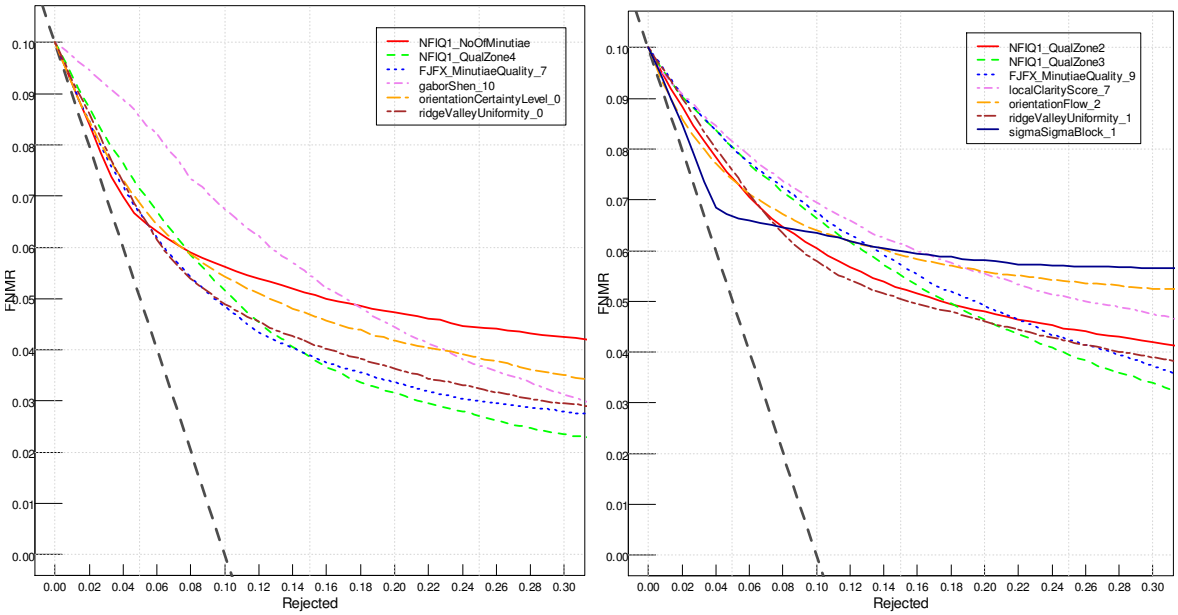

Figure 34: Best features in ERC at 10% FNMR for provider 28

4.4.4 Summary

We obtain the following rankings.

Correlation	ROC (28)	ROC (63, 83)	FNMR = 3%	FNMR = 10%
NFIQ1 QZ4	LCS1	LCS1	MMSB	NFIQ1 QZ4
GSh	LCS7	LCS7	NFIQ NoMin	FJFX MinQual7
NFIQ1 QZ3	OCL	OCL	GS9	RVU0
RVU0	GSh	GSh	Mu	OCL
OCL	FJFX MinQual7	NFIQ1 QZ4	MSB	NFIQ1 NoMin
PS	NFIQ1 QZ4	RVU0	SSB	GSh

Correlation	ROC (28)	ROC (63, 83)	FNMR = 3%	FNMR = 10%
RVU1	NFIQ1 QZ3	OF	FJFX MinQual7	RVU1
FJFX MinQual9	MMSB	PS	RVU0	NFIQ1 QZ2
NFIQ1 QZ1	NFIQ1 NoMin	FJFX MinQual7	OCL	NFIQ1 QZ3
NFIQ1 Min05/06	RVU0	MMB	NFIQ1 QZ3	FJFX MinQual9
NFIQ1 Min07	MMB	MMSB	OF	OF
FJFX MinQual7	OF	NFIQ1 QZ3	NFIQ1 QZ4	SSB
FJFXMinQual10	PS	NFIQ1 NoMin	NFIQ1 FG	LCS7

Table 14: Top ranks of ERC evaluation for all features

From the various evaluation methods, we (subjectively) derive a rough ranking of the features (with configuration number indicated) which reflects their priority for consideration in the NFIQ2 training process:

1. NFIQ1 Quality Zone 4
2. FingerJetFX Minutiae Quality 7
3. Orientation Certainty Level 0
4. Ridge Valley Uniformity 0
5. Gabor Shen 10
6. NFIQ1 Total # Minutiae
7. Ridge Valley Uniformity 1
8. Mu Mu Sigma Block 0
9. Local Clarity Score 7
10. NFIQ1 Quality Zone 3
11. FingerJetFX Minutiae Quality 9
12. Power Spectrum 0
13. Sigma Sigma Block 0
14. Gabor Segement 9
15. Mu Sigma Block 0
16. Local Clarity Score 1
17. FingerJetFX Minutiae Quality 10
18. FingerJetFX Minutiae Quality 6
19. Orientation Flow 2
20. Mu Mu Block
21. NFIQ1 Foreground
22. Gabor 0
23. FingerJetFX Minutiae Quality 8
24. Freqeuncy Domain Analysis 1

5 References

[1] M. S. Altarawneh, W. L. Woo, and S. S. Dlay: "Objective fingerprint image quality assessment using gabor spectrum approach", In Proc. 15th Int Digital Signal Processing Conf, pp. 248–251, 2007.

[2] R. Bolle, S. Pankanti, Y.-S. Yao: "System and Method for Determining the Quality of Fingerprint Images", US Patent Number US 596356, 1999.

[3] Y. Chen, S. Dass, and A. Jain: "Fingerprint quality indices for predicting authentication performance", In Proc. AVBPA, LNCS-3546, Springer, pp. 160–170, 2005.

[4] L. Hong, Y. Wan, A.K. Jain: "Fingerprint image enhancement: algorithm and performance evaluation", IEEE Transaction on Pattern Analysis and Machine Intelligence 20 (8), pp. 777–789, 1998.

[5] ISO/IEC: "ISO/IEC 29794-1 — Information technology — Biometric sample quality — Part 1: Framework", 2009.

[6] ISO/IEC: "ISO/IEC 29794-4 — Information technology — Biometric sample quality — Part 4: Fingerprint image data", 2010.

[7] E. Lim, X. Jiang, W. Yau, "Fingerprint quality and validity analysis", In Proc. IEEE Int. Conf. Image Processing (ICIP 2002), pp. 22–25, 2002.

[8] J. Merkle, M.Schwaiger: "Development of the NFI 2.0 – Specification of Utility Estimation Module NFIQ2_NFIQplusUtility", BSI, NIST, secunet, hda and Fraunhofer IGD. Version 0.4, 2011.

[9] J. Merkle, M. Schwaiger, M. Breitenstein, O. Bausinger, K. Elwart, M. Nuppeney: „Towards Improving the NIST Fingerprint Image Quality (NFIQ) Algorithm", Proceeding of BIOSIG 2010, Lecture Notes in Informatics, GI, 2010.

[10] N.K. Ratha, R.M. Bolle: "Fingerprint Image Quality Estimation", IBM Computer Science Research Report RC 21622, 1999.

[11] L.L. Shen, A. Kot, W.M. Koo: "Quality measures of fingerprint images", Proc. 3rd International Conference Audio- and Video-based Biometric Person Authentication (AVBPA 2001), pp. 182–271, 2001.

[12] E. Tabassi, C. Wilson, C. Watson: „Fingerprint Image Quality," NIST Internal Report 7151, August 2004. http://fingerprint.nist.gov/NBIS.

[13] C. Watson, M. Garris, E. Tabassi, C. Wilson, R. McCabe, S. Janet, K. Ko: „User's Guide to NIST Biometric Image Software (NBIS)", NIST, 2006, http://fingerprint.nist.gov/NFIS/

[14] E.-K. Yun, S.-B. Cho: "Adaptive fingerprint image enhancement with fingerprint image quality analysis". Image Vision Comput. 24 (1), pp. 101-110, 2006.